

Results of Green's function Monte Carlo calculations in the quasi-elastic sector

Alessandro Lovato

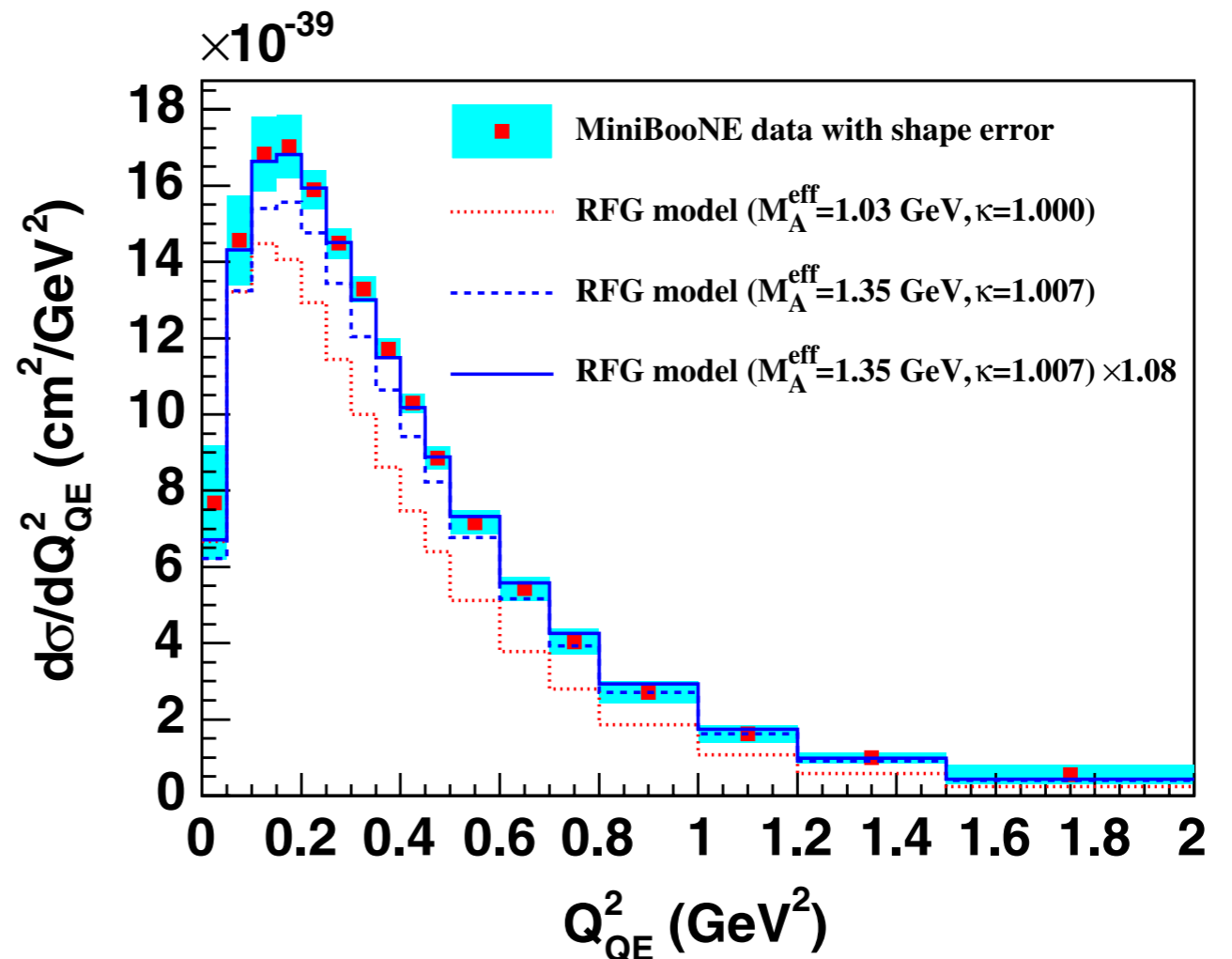
In collaboration with:

Omar Benhar, Stefano Gandolfi, Joe Carlson, Steve Pieper, Noemi Rocco, and Rocco Schiavilla



Why quantum Monte Carlo?

- The Relativistic Fermi gas model is not adequate to account for both the complexity of nuclear dynamics and the variety of reaction mechanisms contributing to the observed neutrino - nucleus cross section
- Quantum Monte Carlo (QMC) can be exploited to compute the electroweak response fully taking into account the correlations induced by the nuclear interactions and meson-exchange currents
- Neutrino experimental communities need accurate theoretical calculations, with reliable error estimates
- QMC methods allow for solving the time-independent Schrödinger equation for nuclear Hamiltonians and naturally provide estimates of the gaussian error of the calculation.



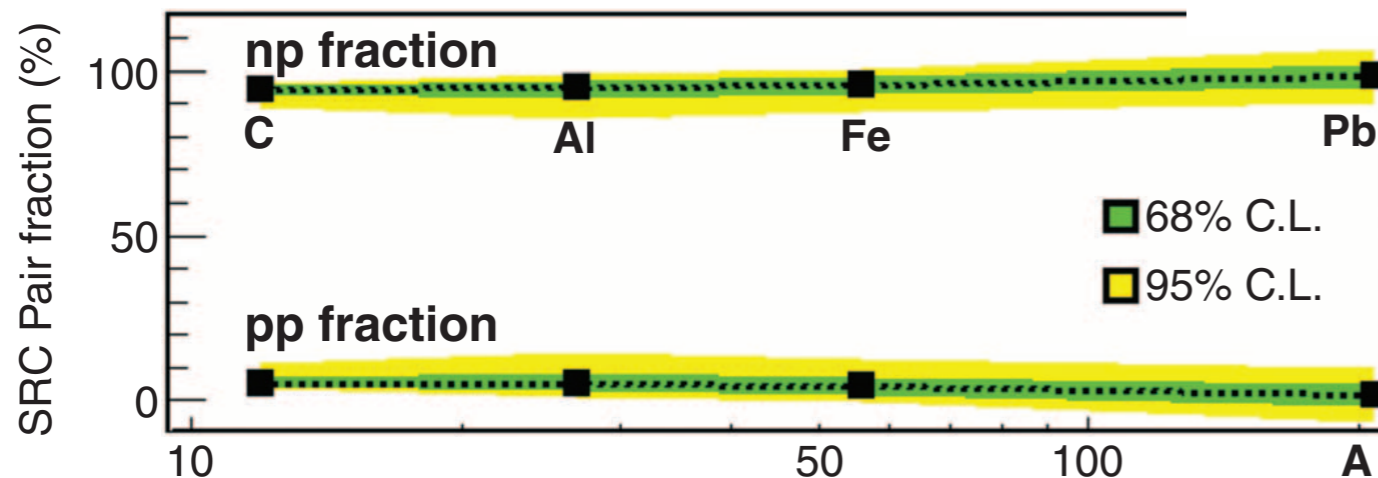
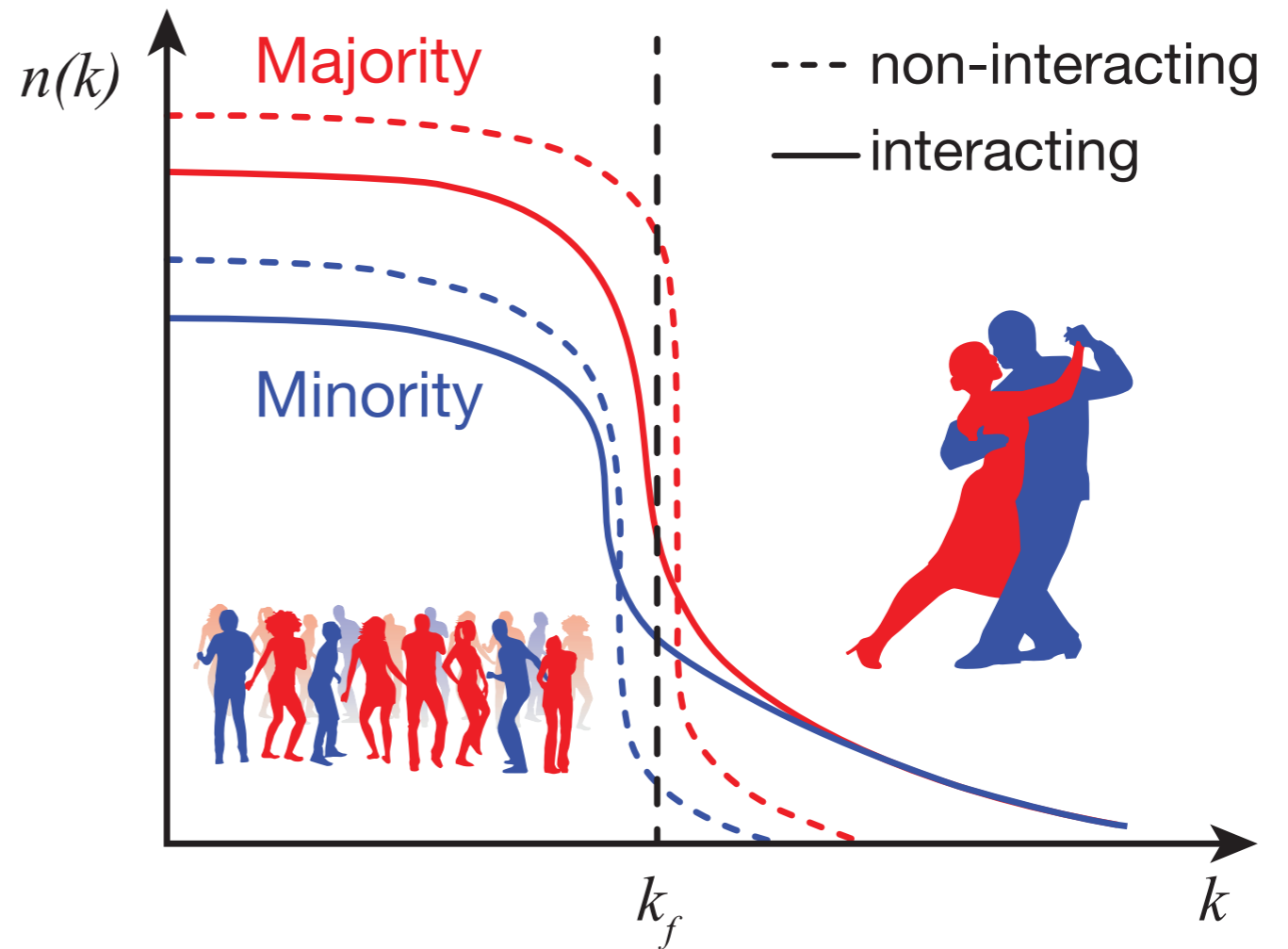
Electron scattering data

- A large body of experimental data for the electromagnetic response of ^4He and ^{12}C (and larger nuclei) is available.
- A model unable to describe electron-nucleus scattering is (very) unlikely to describe neutrino-nucleus scattering.
- Electron-scattering has also provided evidence of the existence of short-range nucleon-nucleon correlations



Nuclear correlations

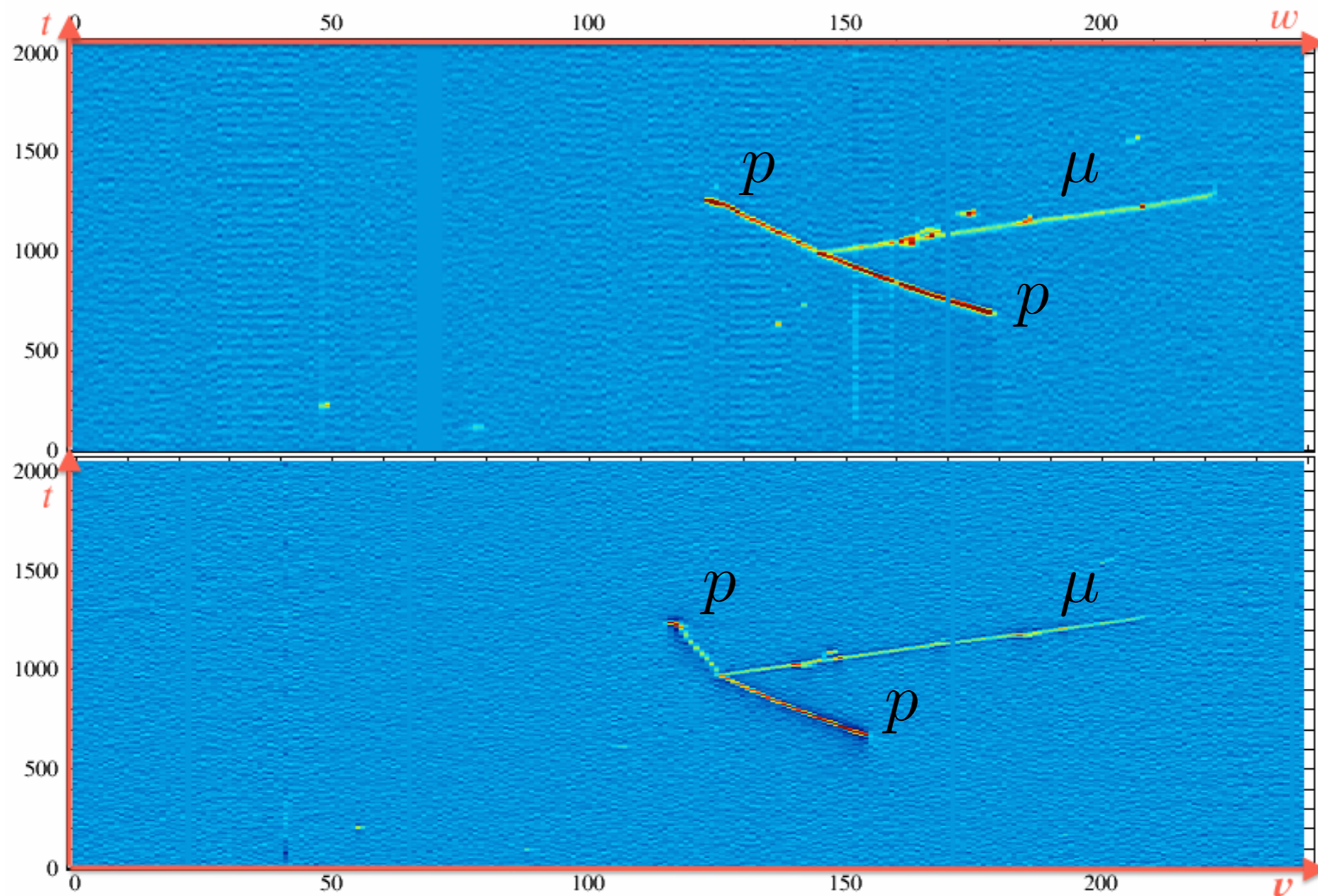
- Nuclear interaction creates short-range correlated pairs of unlike fermions with large relative momentum and pushes fermions from low momenta to high momenta creating a “high-momentum tail.”
- Like in a dance party with a majority of girls, where boy-girl interactions will make the average boy dance more than the average girl



- Even in neutron-rich nuclei, protons have a greater probability than neutrons to have momentum larger than the Fermi momentum.

Nuclear correlations

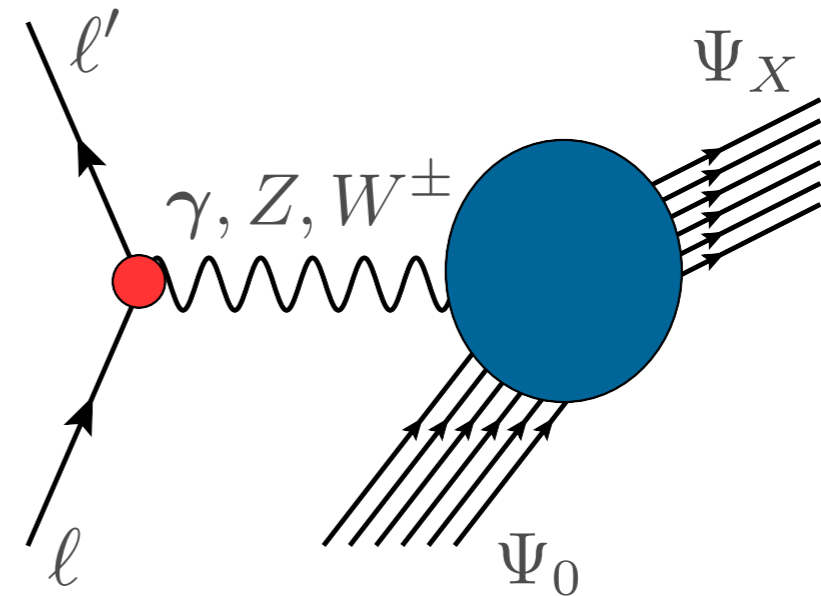
- Recently, evidence of nuclear correlations has been also found in neutrino-nucleus scattering events by the ArgoNeuT experiment at Fermilab.



Lepton-nucleus scattering

The inclusive cross section of the process in which a lepton scatters off a nucleus and the hadronic final state is undetected can be written as

$$\frac{d^2\sigma}{d\Omega_\ell dE_{\ell'}} = L_{\mu\nu} W^{\mu\nu}$$



- The leptonic tensor $L_{\mu\nu}$ is fully specified by the lepton kinematic variables. For instance, in the electron-nucleus scattering case

$$L_{\mu\nu}^{\text{EM}} = 2[k_\mu k'_\nu + k_\nu k'_\mu - g_{\mu\nu}(kk')]$$

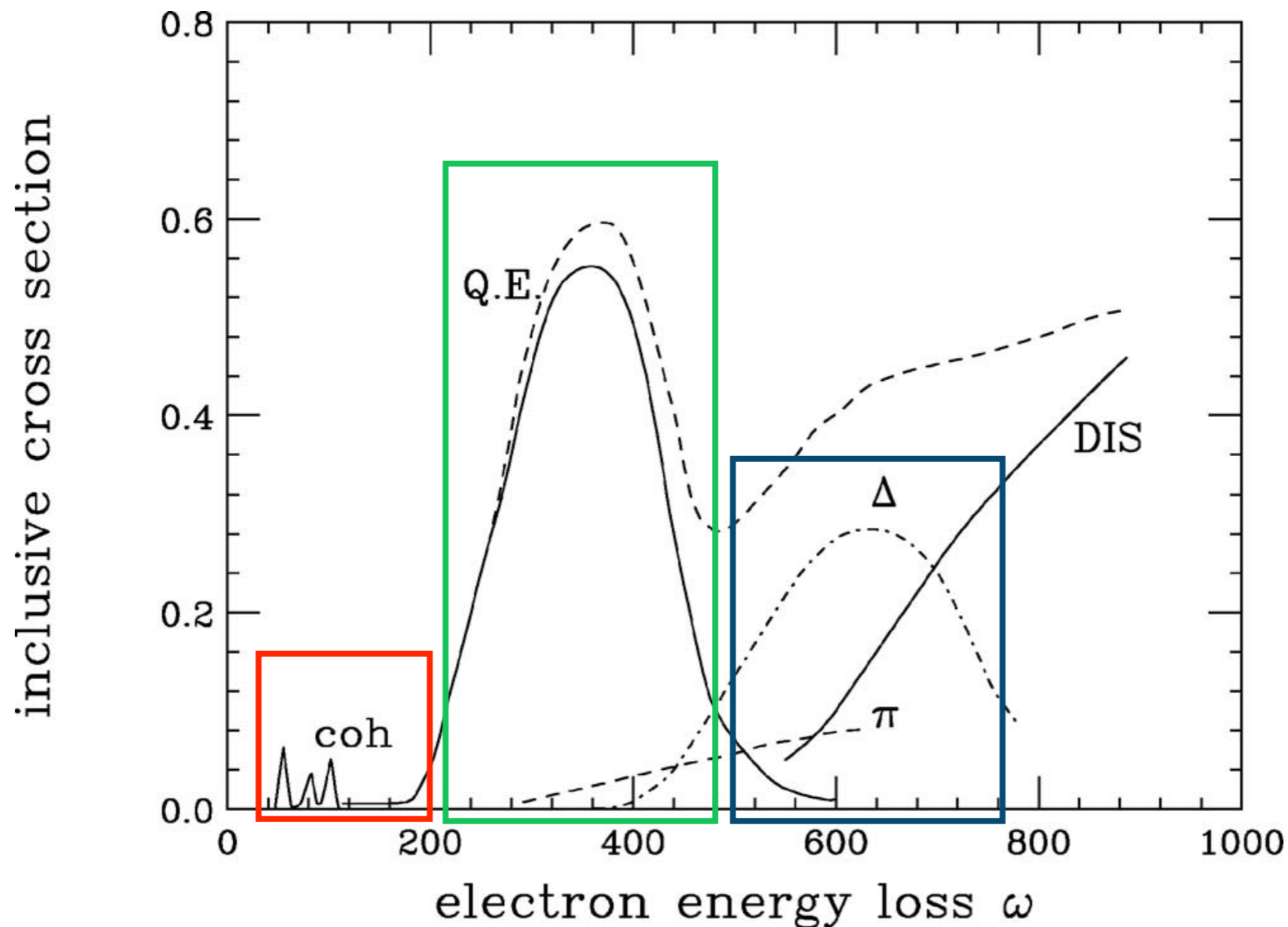
- The Hadronic tensor contains all the information on target response

$$W^{\mu\nu} = \sum_X \langle \Psi_0 | J^{\mu\dagger}(q) | \Psi_X \rangle \langle \Psi_X | J^\nu(q) | \Psi_0 \rangle \delta^{(4)}(p_0 + q - p_X)$$

Note that the initial state does not depend on the momentum transfer!

Electron-nucleus scattering

Schematic representation of the inclusive cross section as a function of the energy loss.



- Elastic scattering and inelastic excitation of discrete nuclear states.
- Broad peak due to quasi-elastic electron-nucleon scattering.
- Excitation of the nucleon to distinct resonances (like the Δ) and pion production.

Towards a unified approach

Moderate momentum transfer regime

- *Ab initio* Green's Function Monte Carlo calculation of the nuclear response from threshold up to the quasielastic region, initially for nuclei as large as ^{12}C .

Large momentum transfer regime

- Development and implementation of the factorization approximation, in which the hadronic final state is written as a product of a state representing the high-momentum particles produced in the interaction process, and a state representing the spectator nucleons, described by spectral functions.

Both approaches are based on the same dynamical framework: the nucleus consists of a collection of A non relativistic nucleons the dynamics of which being described by

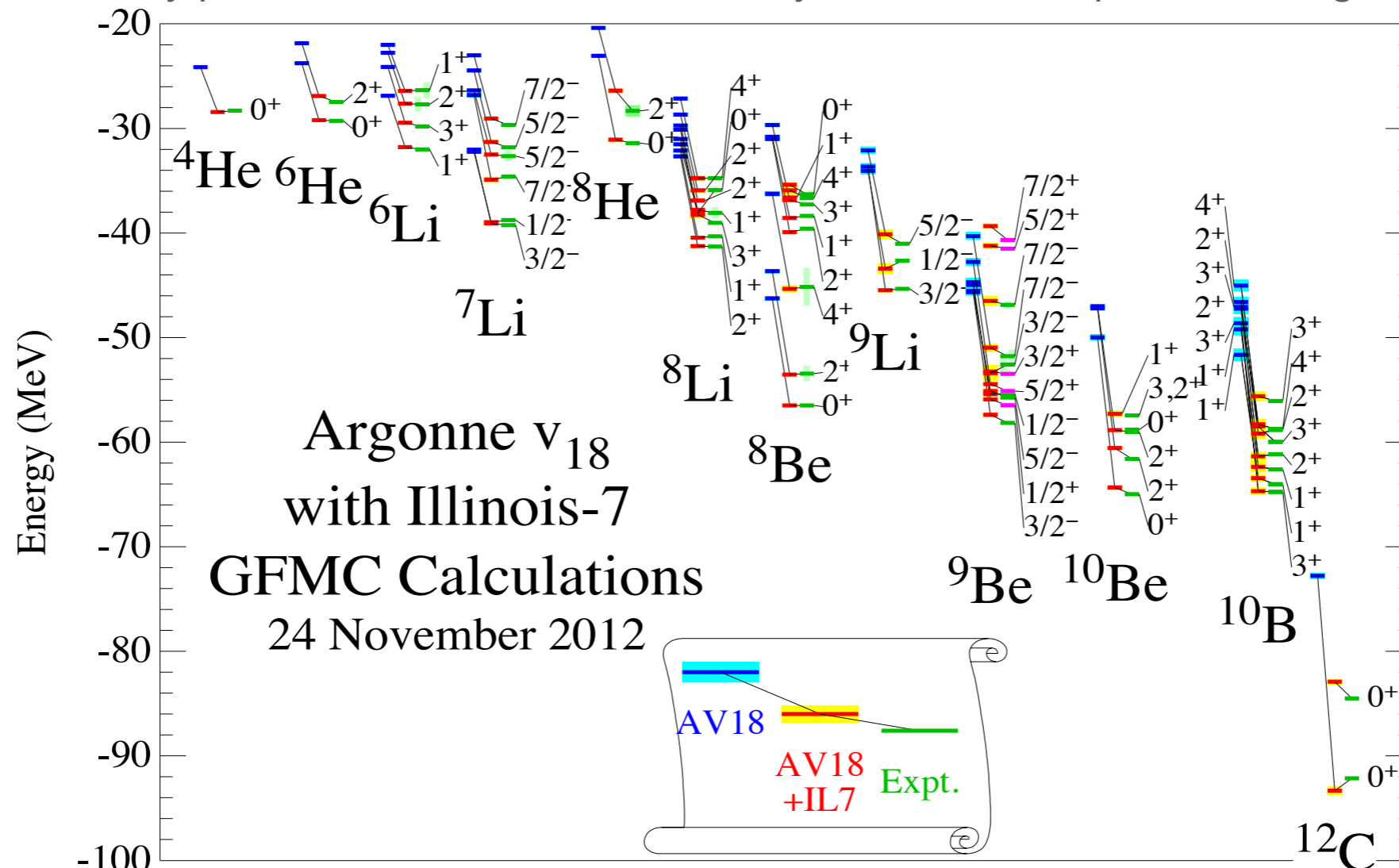
$$H = \sum_i \frac{\mathbf{p}_i^2}{2m} + \sum_{i < j} v_{ij} + \sum_{i < j < k} V_{ijk} + \dots \quad H|\Psi_0\rangle = E_0|\Psi_0\rangle$$

Nuclear hamiltonian

- Argonne v₁₈ two-body potential reproduces the ~4300 np and pp scattering data below 350 MeV of the Nijmegen database with $\chi^2 \simeq 1$.

Definition: *ab initio* approaches are those which rely on the thousands of NN scattering data

- Illinois 7 three-body potential is needed to accurately describe the spectrum of light nuclei

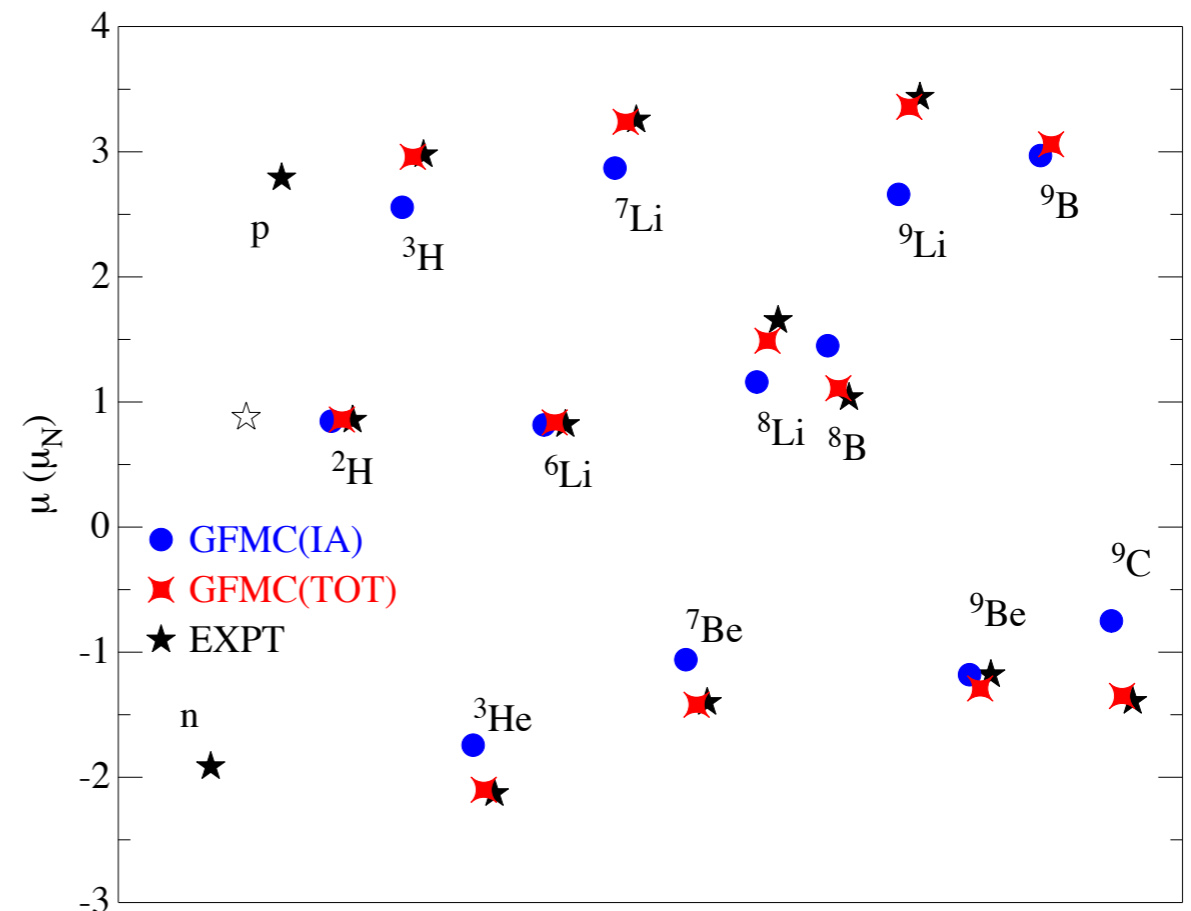
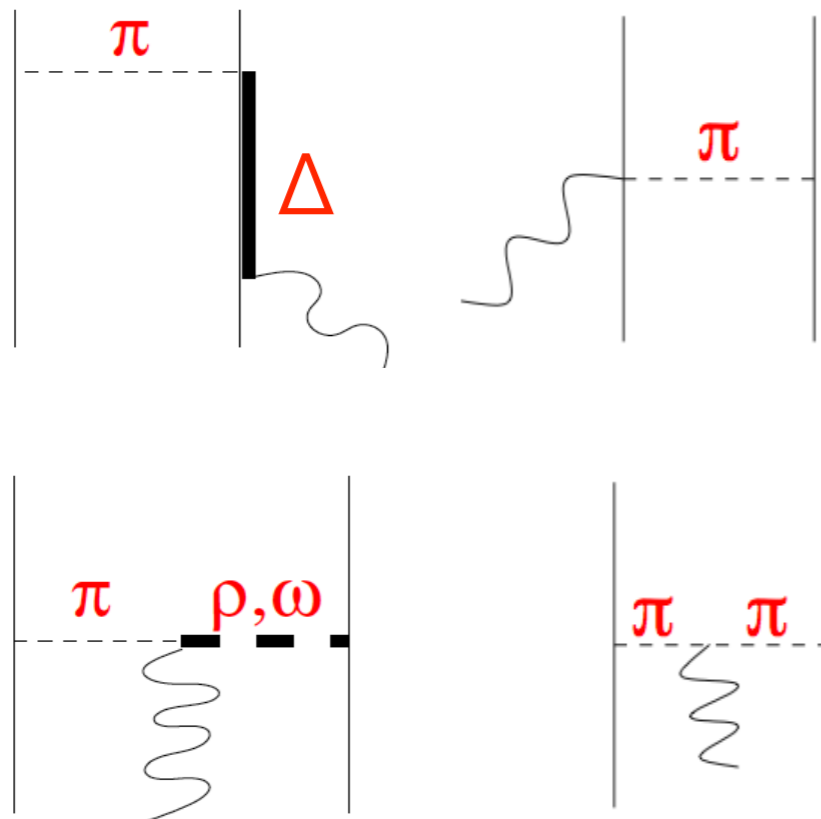


Nuclear currents

The nuclear electromagnetic current is constrained by the Hamiltonian through the continuity equation

$$\nabla \cdot \mathbf{J}_{\text{EM}} + i[H, J_{\text{EM}}^0] = 0$$

- Because the NN potential does not commute with the charge operator, the above equation implies that \mathbf{J}_{EM} involves two-nucleon contributions. They account for processes in which the vector boson couples to the currents arising from meson exchange between two interacting nucleons.
- The inclusion of two-body currents is essential for low-momentum and low-energy transfer transitions.



Green's Function Monte Carlo

- The **Green's function Monte Carlo (GFMC)** method uses a projection technique to enhance the true ground-state component of a starting trial wave function.
- The method relies on the observation that the trial wave function can be expanded in the complete set of eigenstates of the the hamiltonian according to

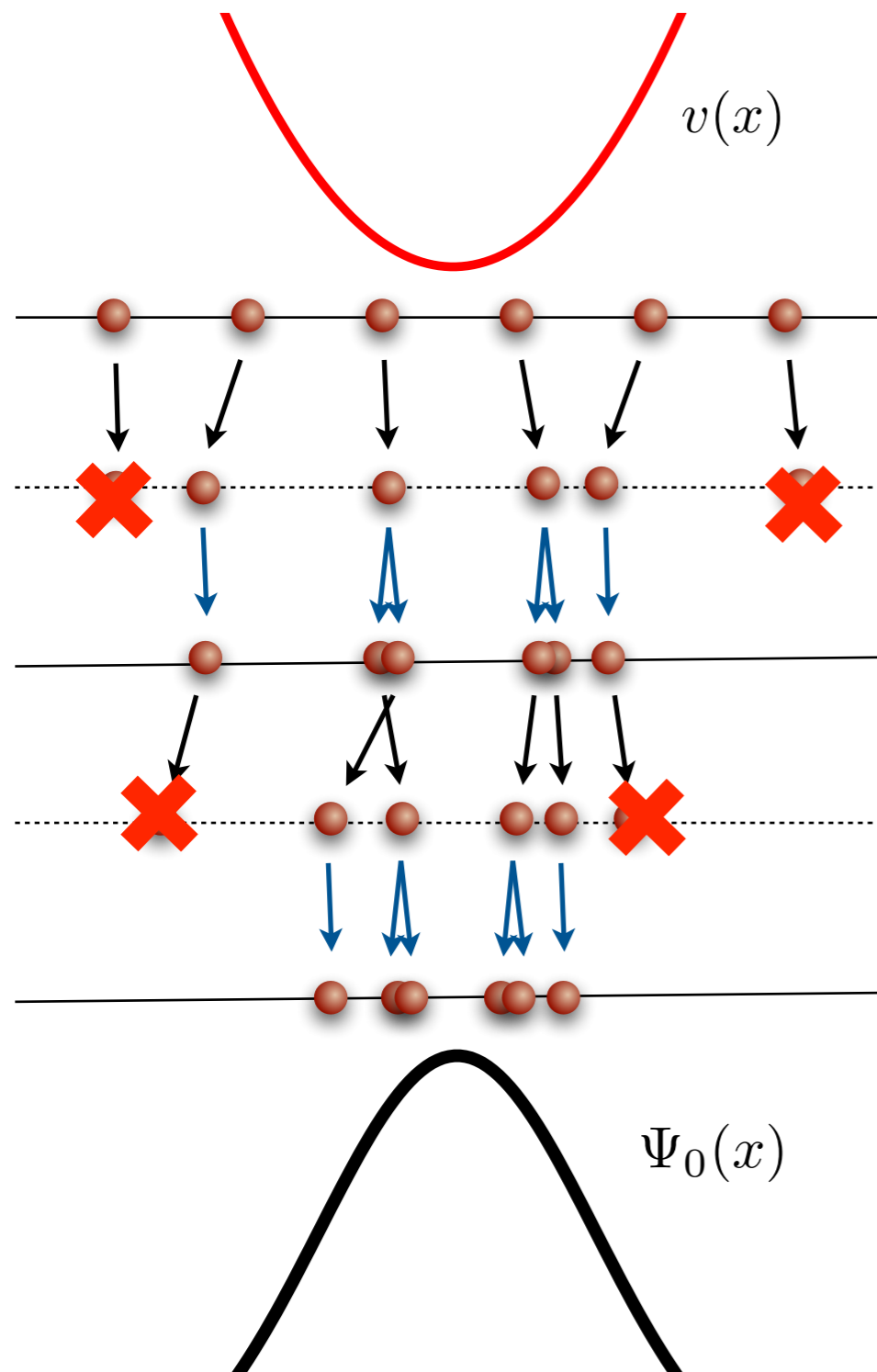
$$|\Psi_T\rangle = \sum_n c_n |\Psi_n\rangle \qquad H|\Psi_n\rangle = E_n |\Psi_n\rangle$$

which implies

$$\lim_{\tau \rightarrow \infty} e^{-(H-E_0)\tau} |\Psi_T\rangle = \lim_{\tau \rightarrow \infty} \sum_n c_n e^{-(E_n-E_0)\tau} |\Psi_n\rangle = c_0 |\Psi_0\rangle$$

where τ is the imaginary time. Hence, DMC projects out the exact lowest-energy state, provided the trial wave function it is not orthogonal to the ground state.

Diffusion Monte Carlo



- A set of walkers is sampled from the trial wave function

- Gaussian drift for the kinetic energy

$$\left(\frac{m}{2\pi\hbar^2\Delta\tau} \right)^{\frac{1}{2}} e^{-\frac{m}{2\hbar^2\Delta\tau}(x_i - x_{i+1})^2}$$

- Branching and killing of the walkers induced by the potential weight

$$w(x_{i+1}) = e^{-[V(x_{i+1}) - E_0]\Delta\tau}$$

- Ground-state expectation values are estimated during the diffusion

$$\langle H \rangle = \frac{\sum_{x_i} \langle x_i | H | \Psi_T \rangle w(x_i)}{\sum_{x_i} \langle x_i | \Psi_T \rangle w(x_i)}$$

Nuclear VMC wave function

The trial wave function of the nucleus reflects the complexity of the nuclear potential

It contains 3-body correlations stemming from 3-body potential

$$\Psi_T = \left[1 + \sum_{i < j < k} \tilde{U}_{ijk}^{\text{TNI}} \right] \Psi_P \longleftrightarrow \tilde{U}_{ijk} \equiv \tilde{\epsilon}_A V_{ijk}^A + \tilde{\epsilon}_R V_{ijk}^R$$

The pair correlated wave function is written in terms of operator correlations arising from the 2-body potential

$$\Psi_P = \left[\mathcal{S} \prod_{i < j} (1 + U_{ij}) \right] \Psi_J \longleftrightarrow U_{ij} = \sum_{p=2,6} u^p(r_{ij}) O_{ij}^p$$

The total antisymmetric Jastrow wave function depends on the quantum numbers of the given nucleus

$$\Psi_J = \left[\prod_{i < j < k} f_{ijk}^c \right] \left[\prod_{i < j} f_{ij}^c \right] \Phi_A(J, M, T, T_3)$$

Green's Function Monte Carlo

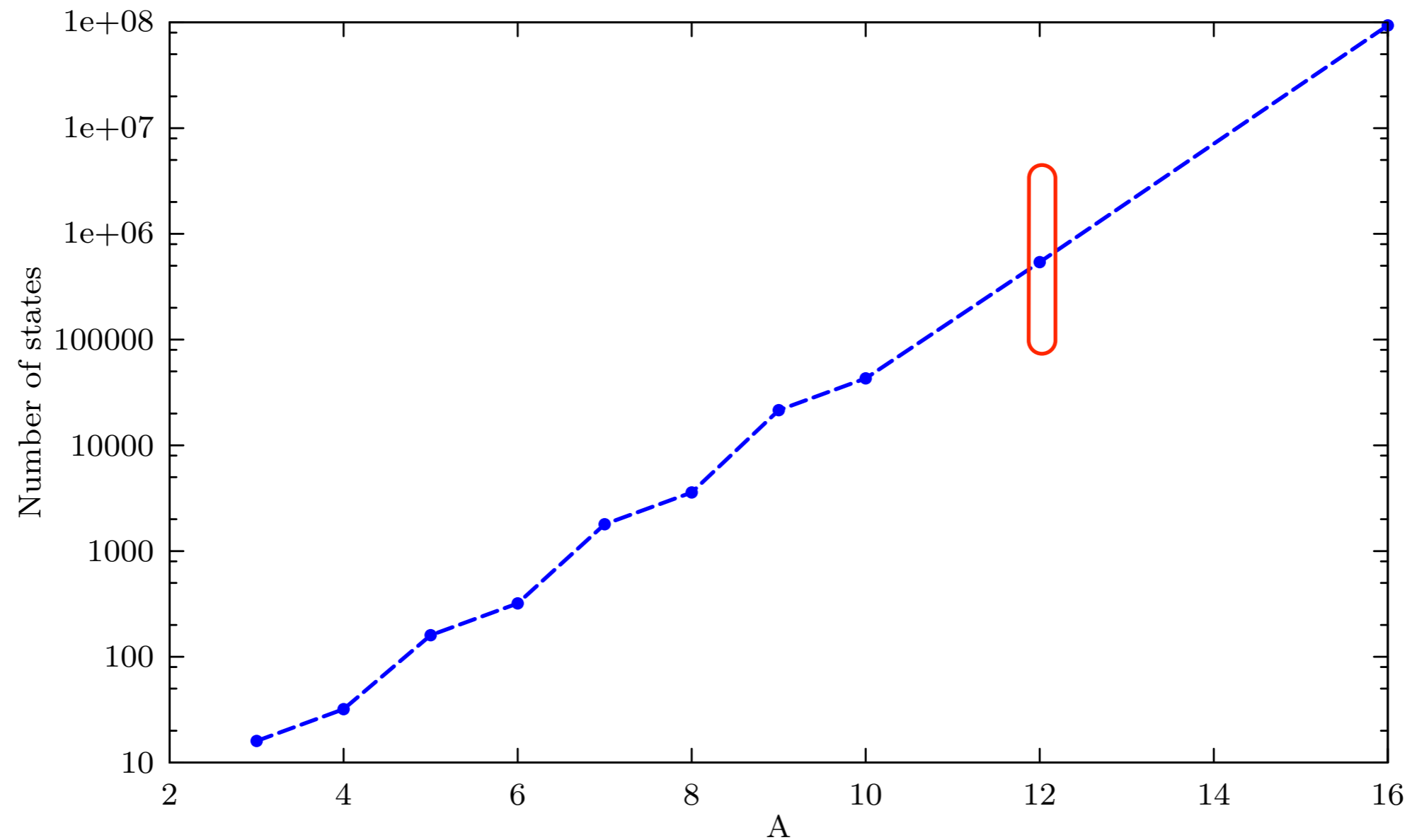
- A walker associated with wave function of the nucleus, do not only describes the positions of the protons and neutrons, but also their spin and isospin!
- The GFMC wave function is written as a complex vector, the coordinates of which represent a spin-isospin state of the system
- The ${}^3\text{H}$ case fits in the slide!

$$|\Psi_{3H}\rangle = \begin{pmatrix} a_{\uparrow\uparrow\uparrow} \\ a_{\uparrow\uparrow\downarrow} \\ a_{\uparrow\downarrow\uparrow} \\ a_{\uparrow\downarrow\downarrow} \\ a_{\downarrow\uparrow\uparrow} \\ a_{\downarrow\uparrow\downarrow} \\ a_{\downarrow\downarrow\uparrow} \\ a_{\downarrow\downarrow\downarrow} \end{pmatrix} \otimes \begin{pmatrix} a_{pnn} \\ a_{npn} \\ a_{nnp} \end{pmatrix}$$

Green's Function Monte Carlo

The number of spin-isospin states grows exponentially with the number of particles

$$N = 2^A \times \binom{A}{Z}$$



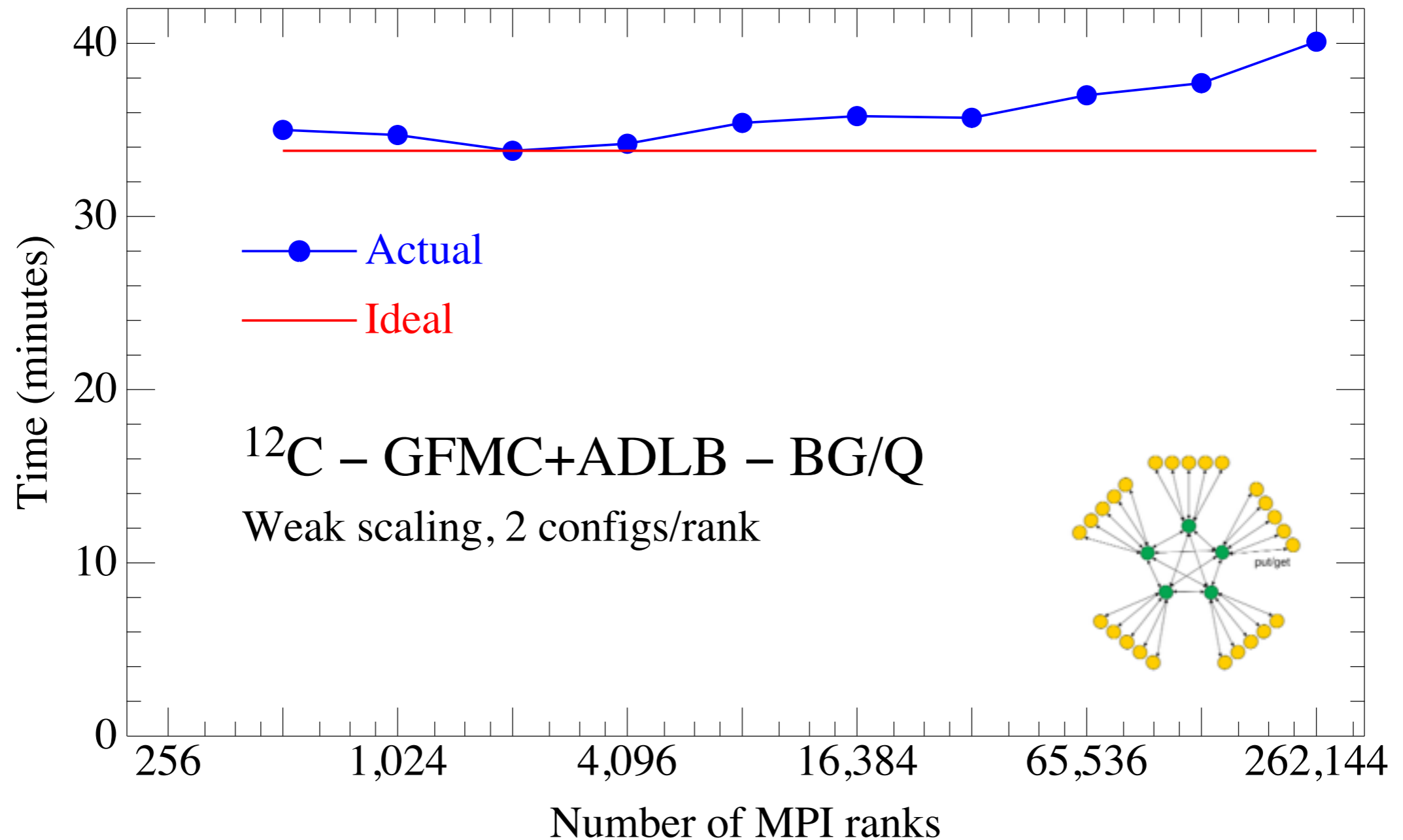
Using supercomputers

- GFMC has steadily undergone development to take advantage of each new generation of parallel machine and was one of the first to deliver new scientific results each time.



Using supercomputers

- GFMC has steadily undergone development to take advantage of each new generation of parallel machine and was one of the first to deliver new scientific results each time.



Moderate momentum transfer regime

Moderate momentum-transfer regime

- At moderate momentum transfer, the inclusive cross section can be written in terms of the response functions

$$R_{\alpha\beta}(\omega, \mathbf{q}) = \sum_f \langle \Psi_0 | J_\alpha^\dagger(\mathbf{q}) | \Psi_f \rangle \langle \Psi_f | J_\beta(\mathbf{q}) | \Psi_0 \rangle \delta(\omega - E_f + E_0)$$

- Both initial and final states are eigenstates of the nuclear Hamiltonian

$$H|\Psi_0\rangle = E_0|\Psi_0\rangle$$

$$H|\Psi_f\rangle = E_f|\Psi_f\rangle$$

- As for the electron scattering on ^{12}C

$$|^{12}\text{C}^*\rangle, |^{11}\text{B}, p\rangle, |^{11}\text{C}, n\rangle, |^{10}\text{B}, pn\rangle, |^{10}\text{B}, pp\rangle \dots$$

These are eigenstate of a bare nuclear Hamiltonian and are, in principle, observable

- Relativistic corrections are included in the current operators and in the nucleon form factors

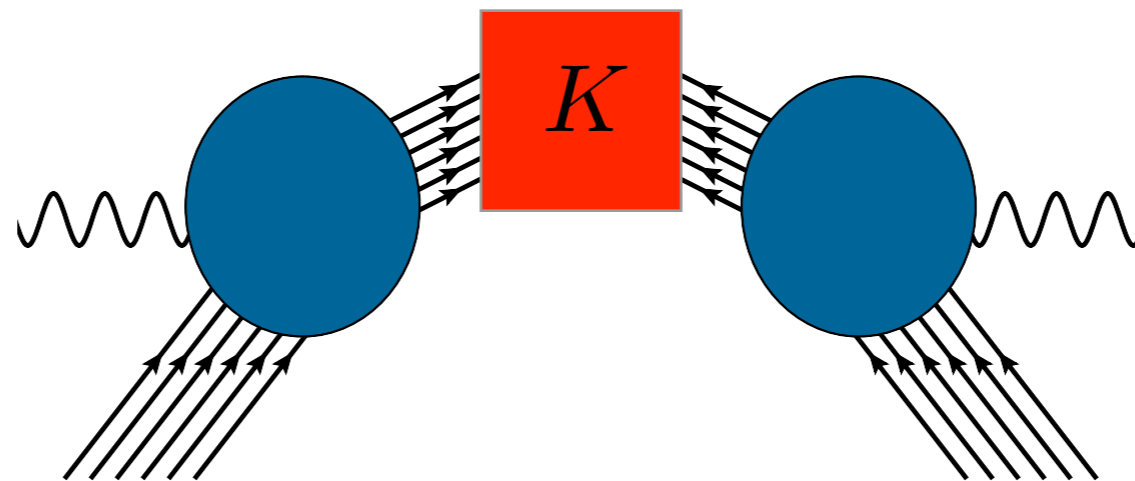
Integral transform techniques

- The integral transform of the response function are generally defined as

$$E_{\alpha\beta}(\sigma, \mathbf{q}) \equiv \int d\omega K(\sigma, \omega) R_{\alpha\beta}(\omega, \mathbf{q})$$

- Using the completeness of the final states, they can be expressed in terms of ground-state expectation values

$$E_{\alpha\beta}(\sigma, \mathbf{q}) = \langle \Psi_0 | J_{\alpha}^{\dagger}(\mathbf{q}) K(\sigma, H - E_0) J_{\beta}(\mathbf{q}) | \Psi_0 \rangle$$

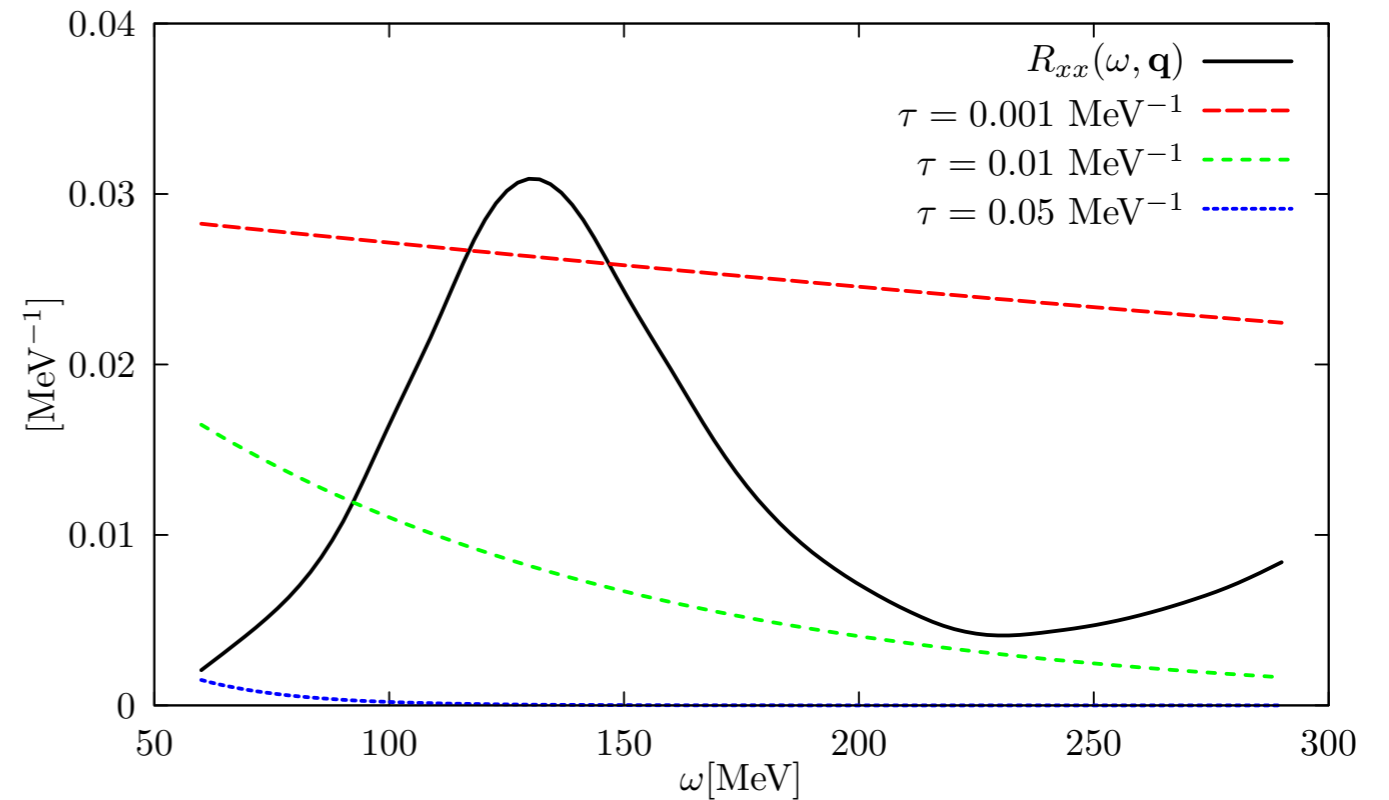


Euclidean response function

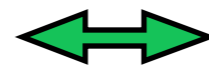
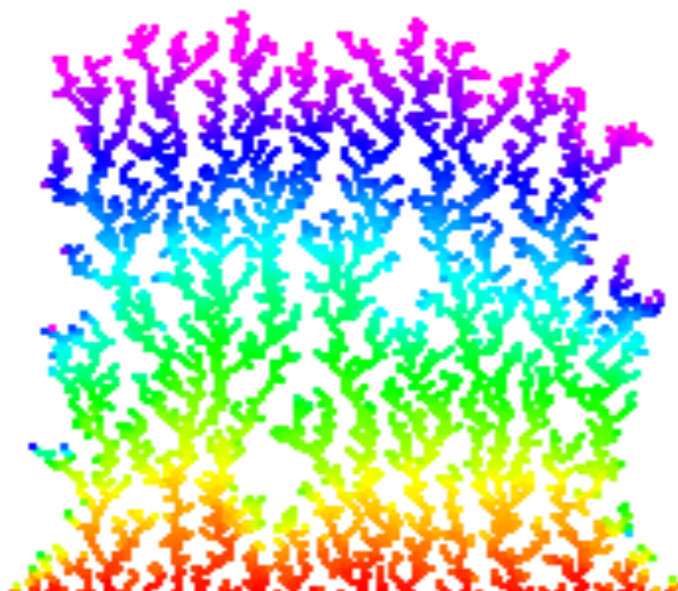
The the Kernel of the Euclidean response defines the Laplace transform

$$K(\tau, \omega) = e^{-\tau\omega}$$

At finite imaginary time the contributions from large energy transfer are quickly suppressed



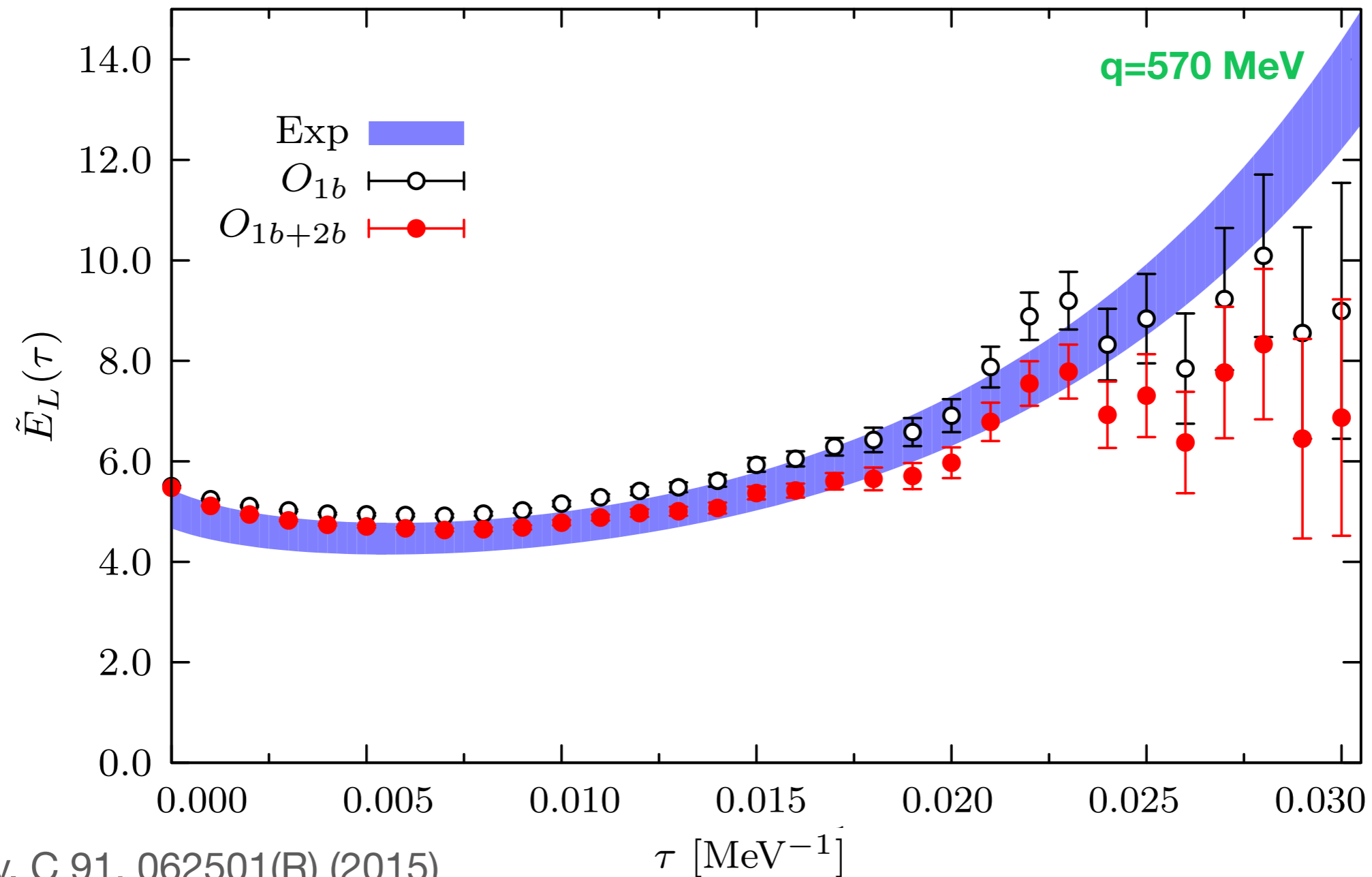
The system is first heated up by the transition operator. How it cools down determines the Euclidean response of the system



$$\frac{\langle \Psi_0 | J_\alpha^\dagger(\mathbf{q}) e^{(H-E_0)\tau} J_\beta(\mathbf{q}) | \Psi_0 \rangle}{\langle \Psi_0 | e^{(H-E_0)\tau} | \Psi_0 \rangle}$$

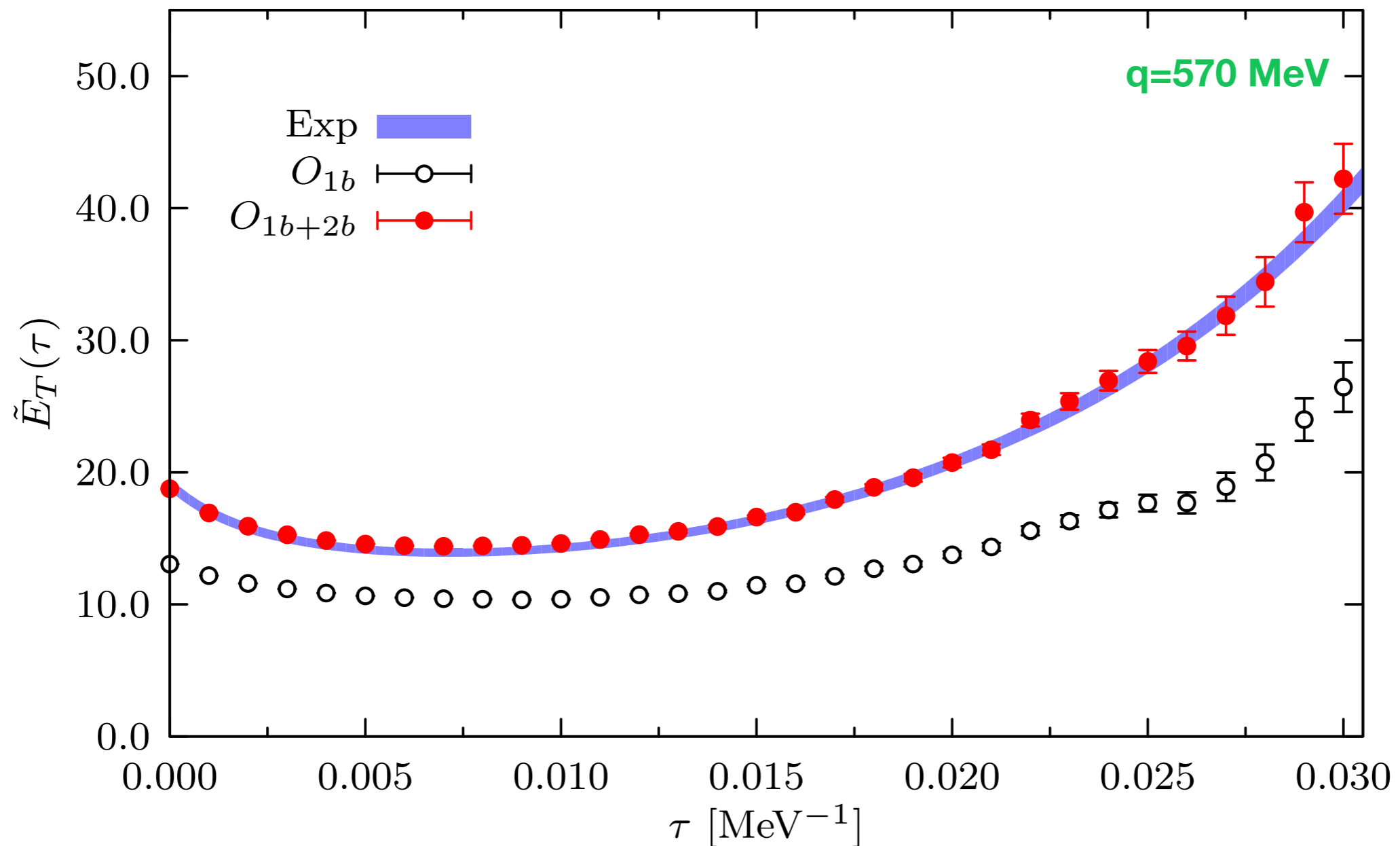
^{12}C electromagnetic Euclidean response

In the electromagnetic longitudinal case, destructive interference between the matrix elements of the one- and two-body charge operators reduces, albeit slightly, the one-body response.



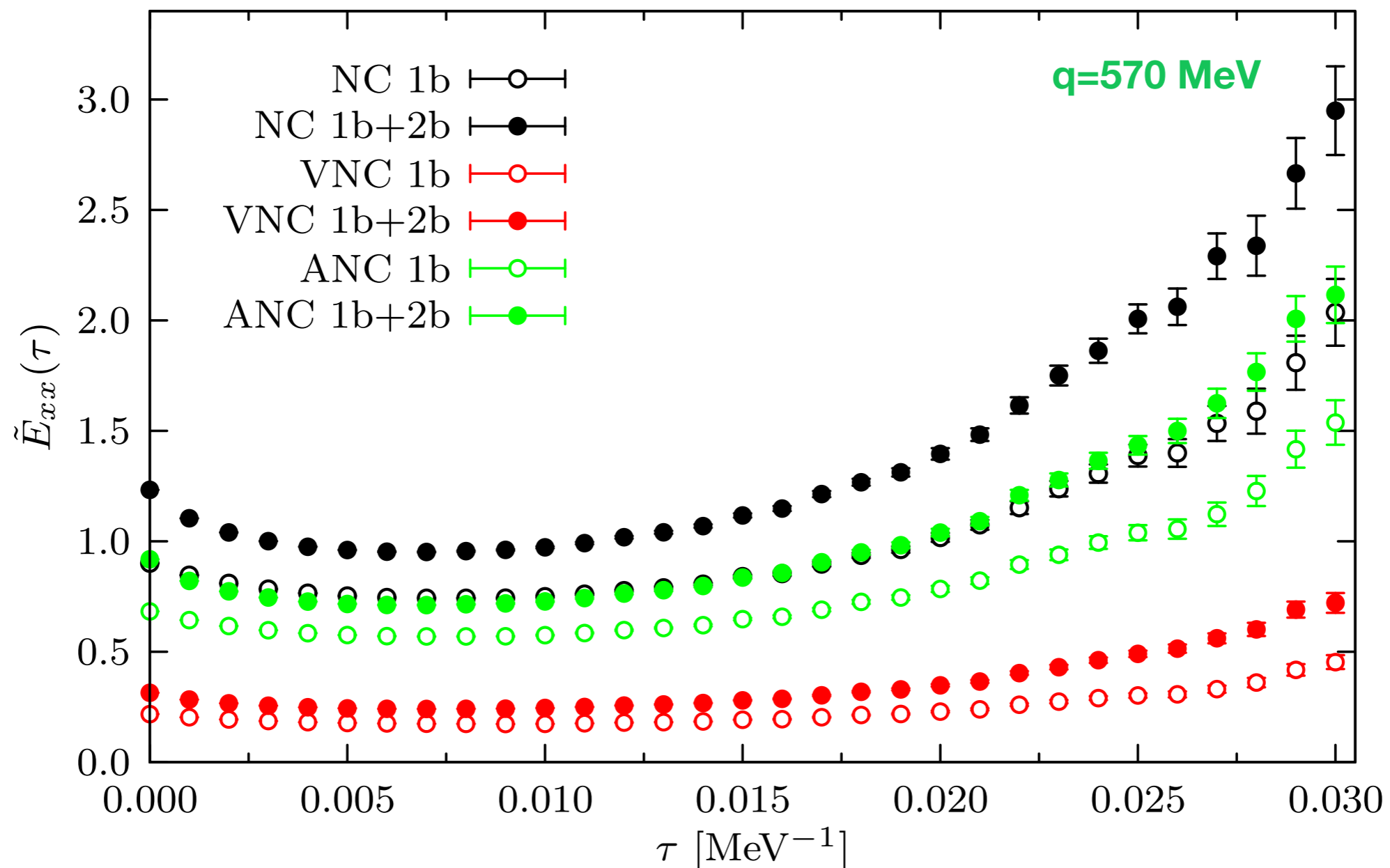
^{12}C electromagnetic Euclidean response

In the electromagnetic transverse case, two-body current contributions substantially increase the one-body response. This enhancement is effective over the whole imaginary-time region we have considered.



^{12}C neutral-current Euclidean response

Both the vector neutral current and the axial neutral current transverse responses are substantially enhanced over the entire imaginary-time region we considered.



Inversion of the Euclidean response

Inverting the Euclidean response is an ill posed problem: any set of observations is limited and noisy and the situation is even worse since the kernel is a smoothing operator.

$$E_{\alpha\beta}(\tau, \mathbf{q}) \longrightarrow R_{\alpha\beta}(\omega, \mathbf{q})$$



Image reconstruction from incomplete and noisy data

S. F. Gull & G. J. Daniell*

Mullard Radio Astronomy Observatory, Cavendish Laboratory, Madingley Road, Cambridge, UK

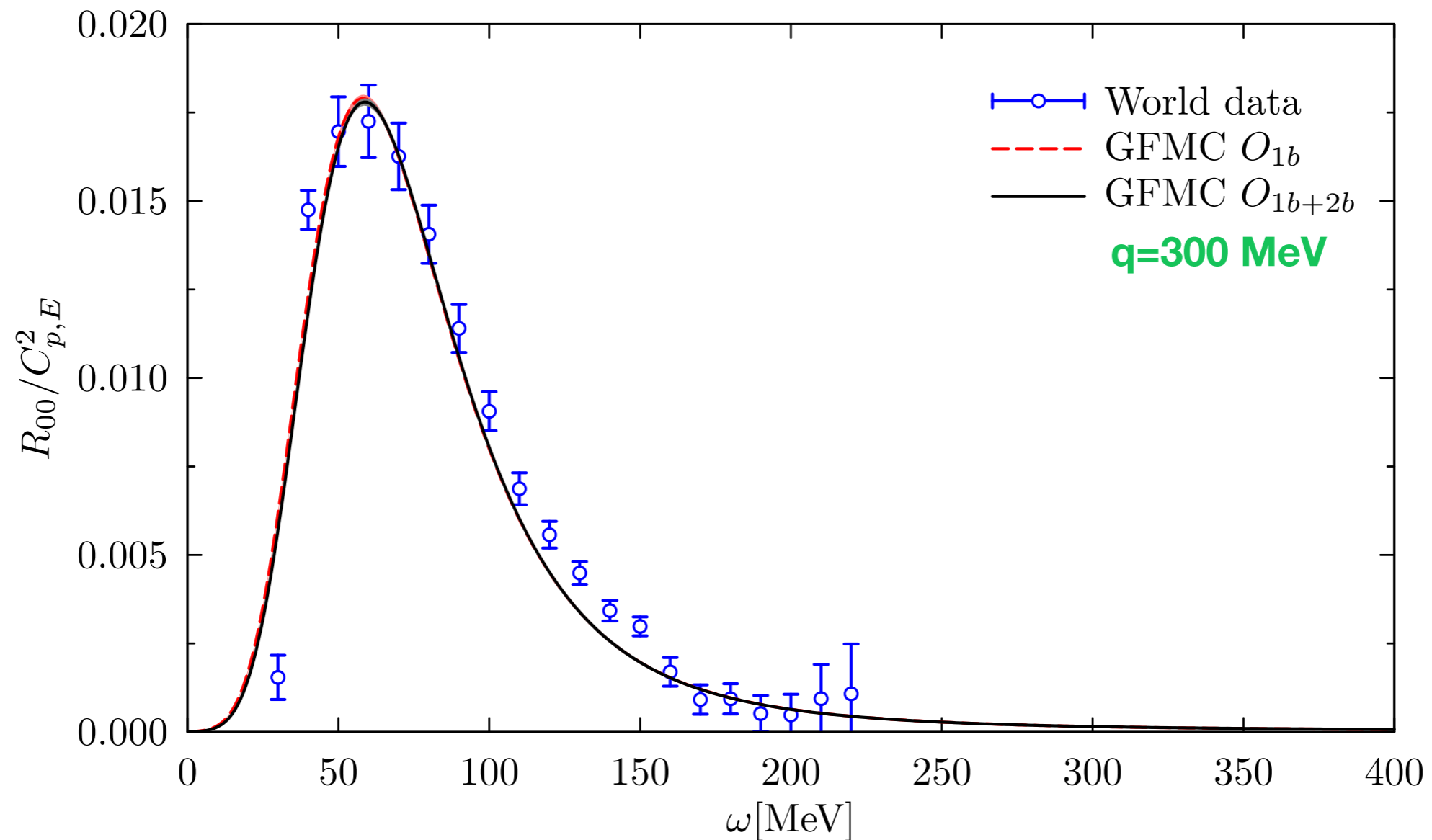
Results are presented of a powerful technique for image reconstruction by a maximum entropy method, which is sufficiently fast to be useful for large and complicated images. Although our examples are taken from the fields of radio and X-ray astronomy, the technique is immediately applicable in spectroscopy, electron microscopy, X-ray crystallography, geophysics and virtually any type of optical image processing. Applied to radioastronomical data, the algorithm reveals details not seen by conventional analysis, but which are known to exist.

To avoid abstraction, we shall refer to our radioastronomical example. Starting with incomplete and noisy data, one can obtain by the Backus–Gilbert method a series of maps of the distribution of radio brightness across the sky, all of which are consistent with the data, but have different resolutions and noise levels. From the data alone, there is no reason to prefer any one of these maps, and the observer may select the most appropriate one to answer any specific question. Hence, the method cannot produce a unique ‘best’ map of the sky. There is no single map that is equally suitable for discussing both accurate flux measurements and source positions.

Nevertheless, it is useful to have a single general-purpose map of the sky, and the maximum-entropy map described here fulfils

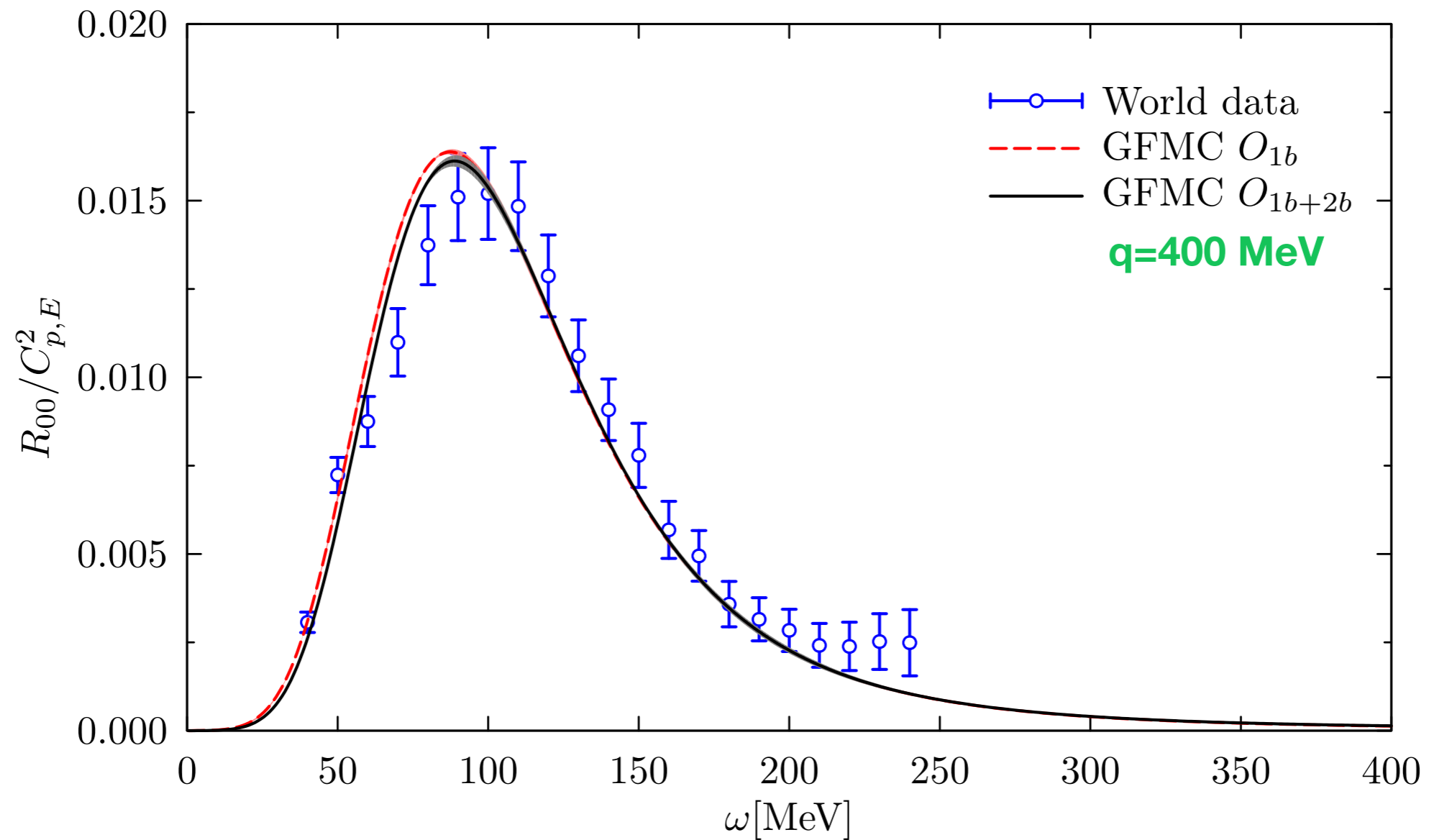
^4He electromagnetic response

Two-body currents do not provide significant changes in the longitudinal response. The agreement with experimental data appears to be remarkably good.



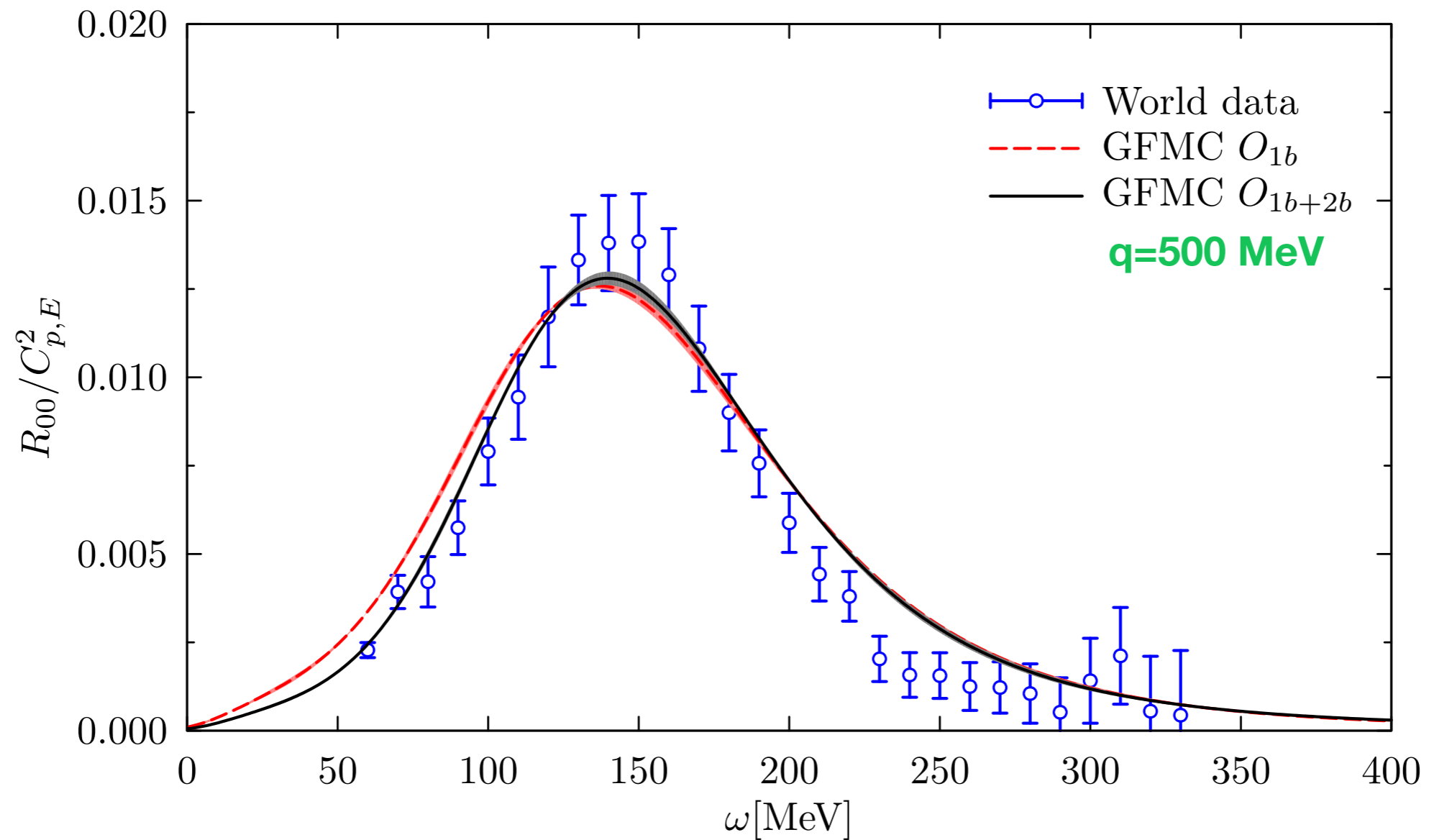
^4He electromagnetic response

Two-body currents do not provide significant changes in the longitudinal response.
The agreement with experimental data appears to be remarkably good.



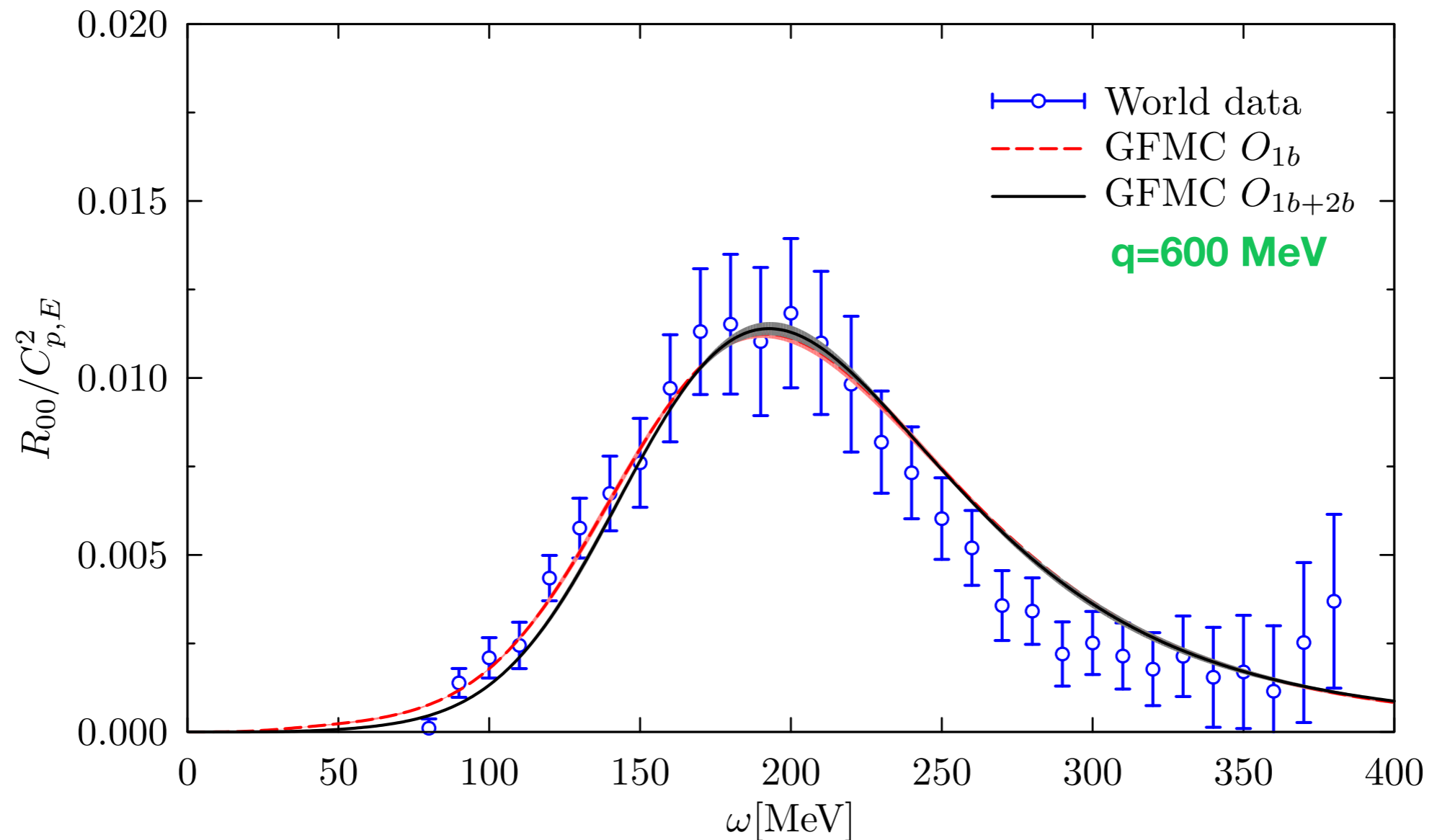
^4He electromagnetic response

Two-body currents do not provide significant changes in the longitudinal response.
The agreement with experimental data appears to be remarkably good.



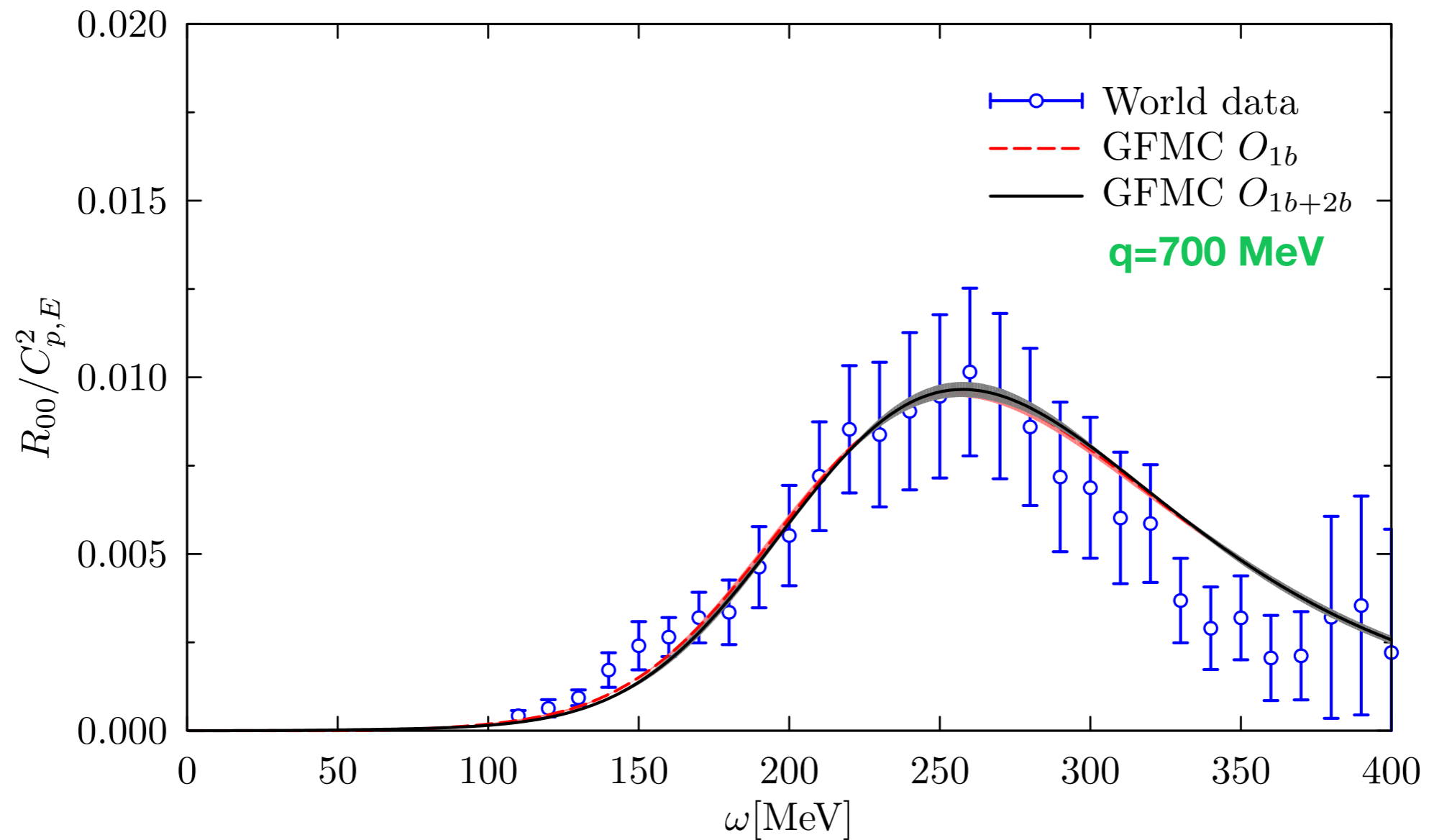
^4He electromagnetic response

Two-body currents do not provide significant changes in the longitudinal response. The agreement with experimental data appears to be remarkably good.



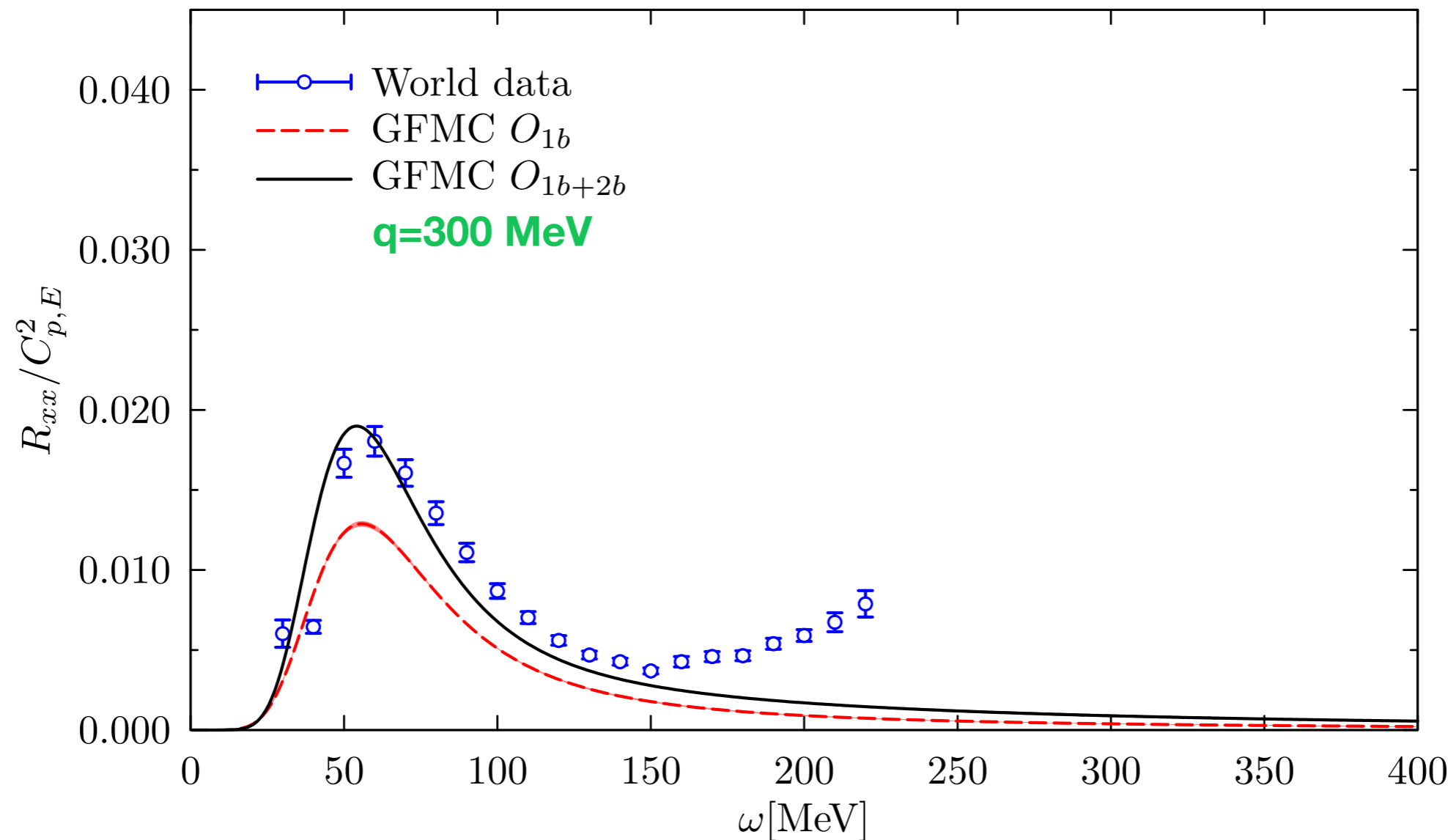
^4He electromagnetic response

Two-body currents do not provide significant changes in the longitudinal response. The agreement with experimental data appears to be remarkably good.



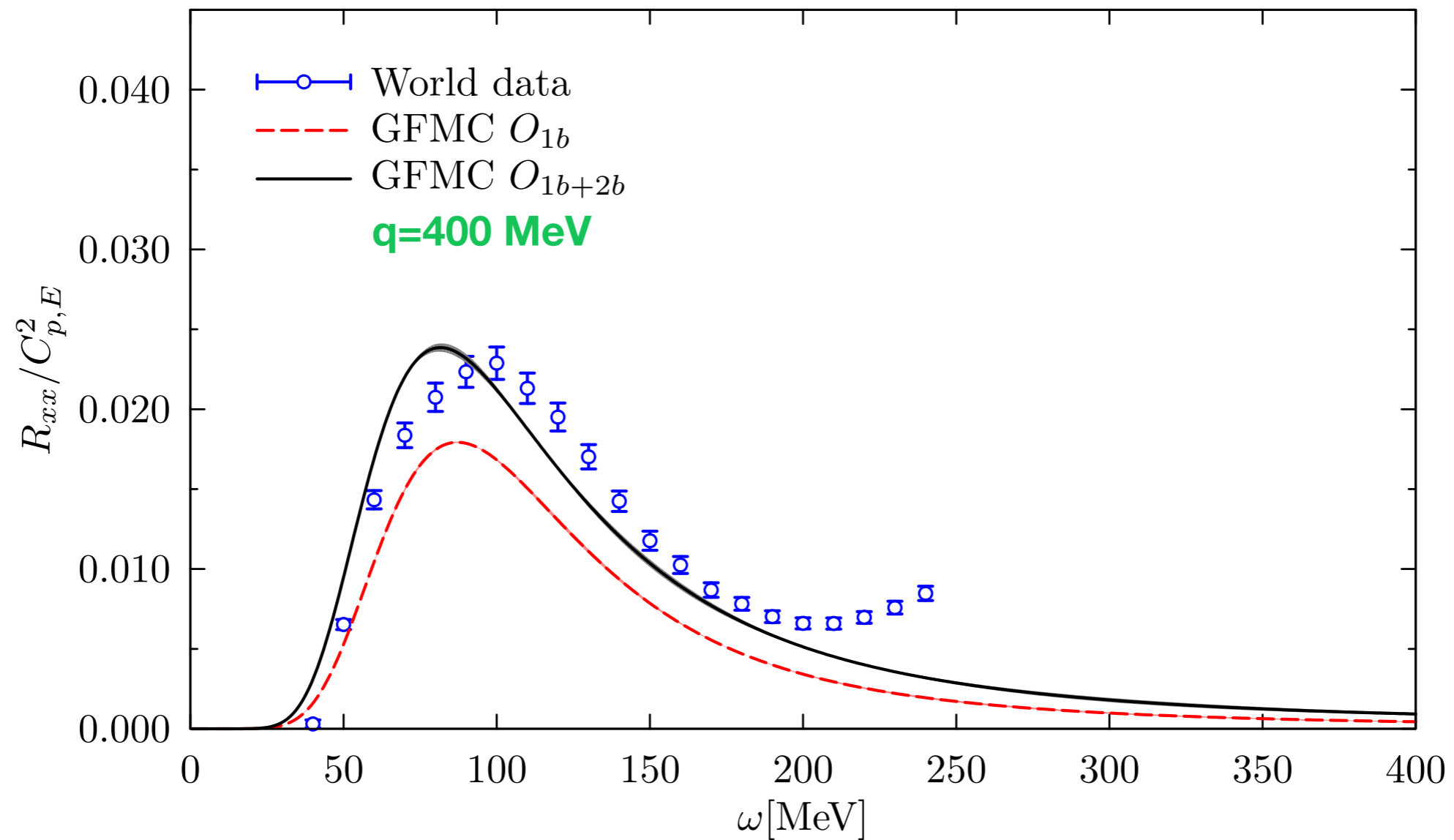
^4He electromagnetic response

Two-body currents significantly enhance the transverse response function, not only in the dip region, but also in the quasielastic peak and threshold regions.



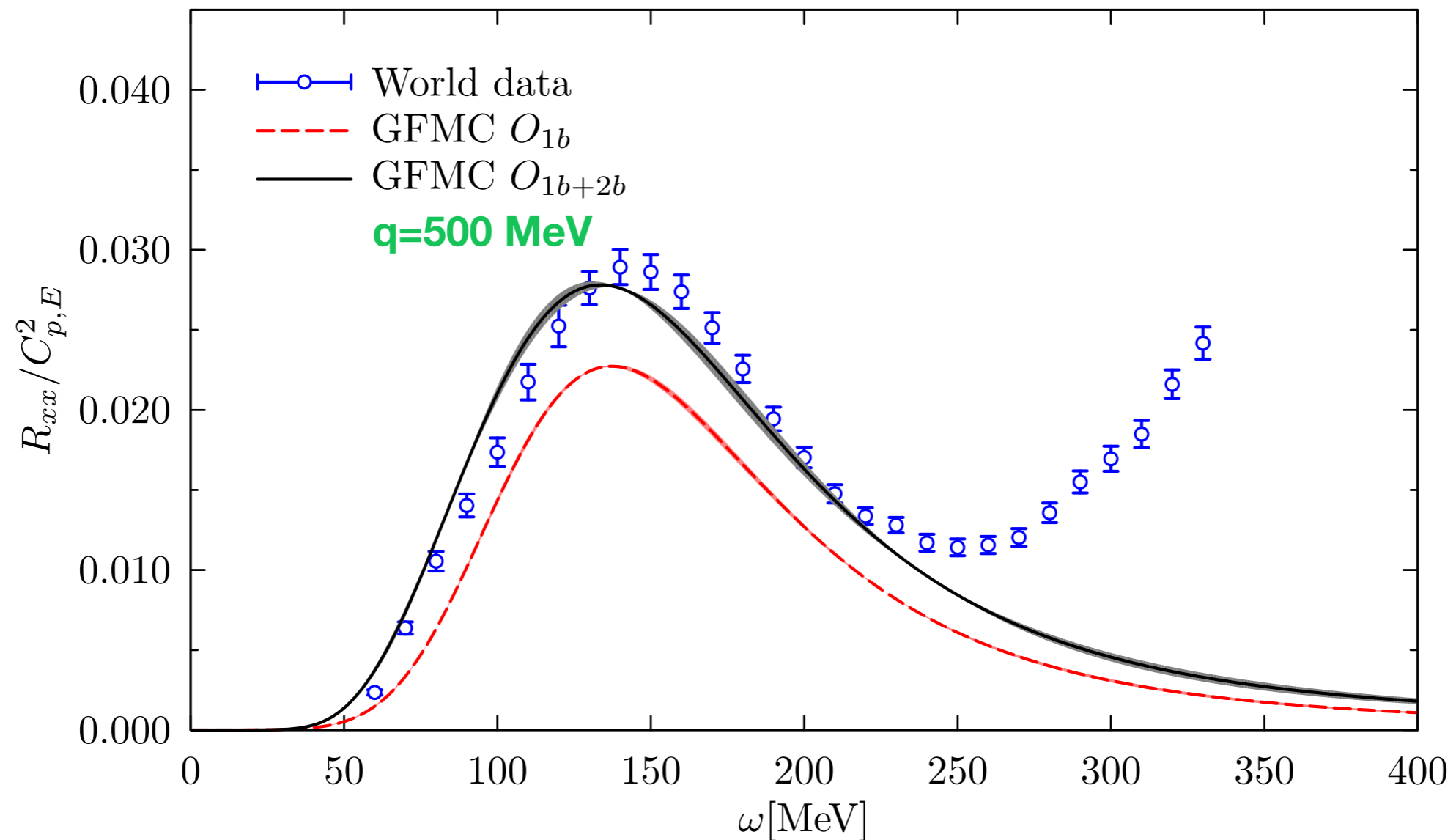
^4He electromagnetic response

Two-body currents significantly enhance the transverse response function, not only in the dip region, but also in the quasielastic peak and threshold regions.



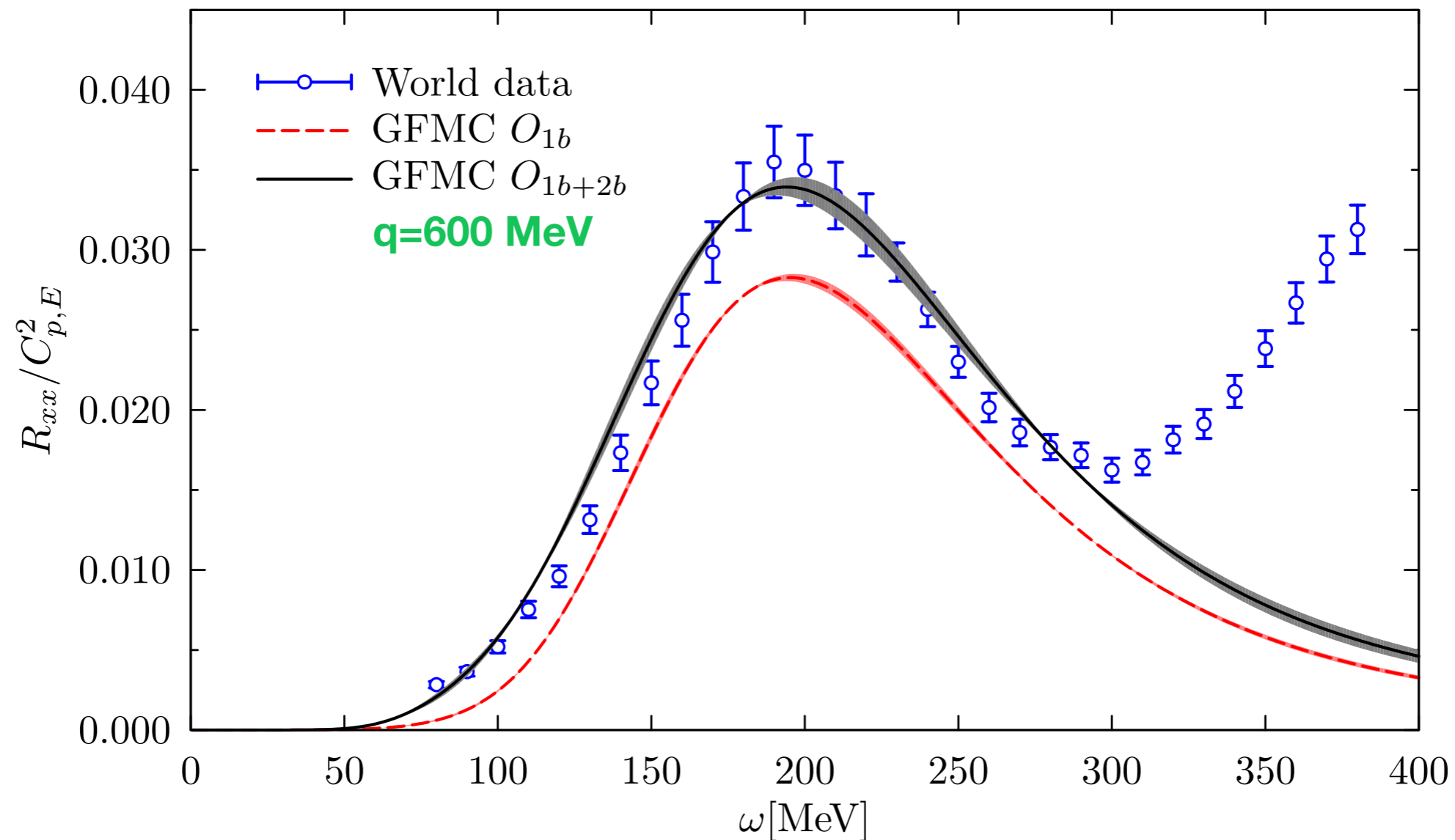
^4He electromagnetic response

Two-body currents significantly enhance the transverse response function, not only in the dip region, but also in the quasielastic peak and threshold regions.



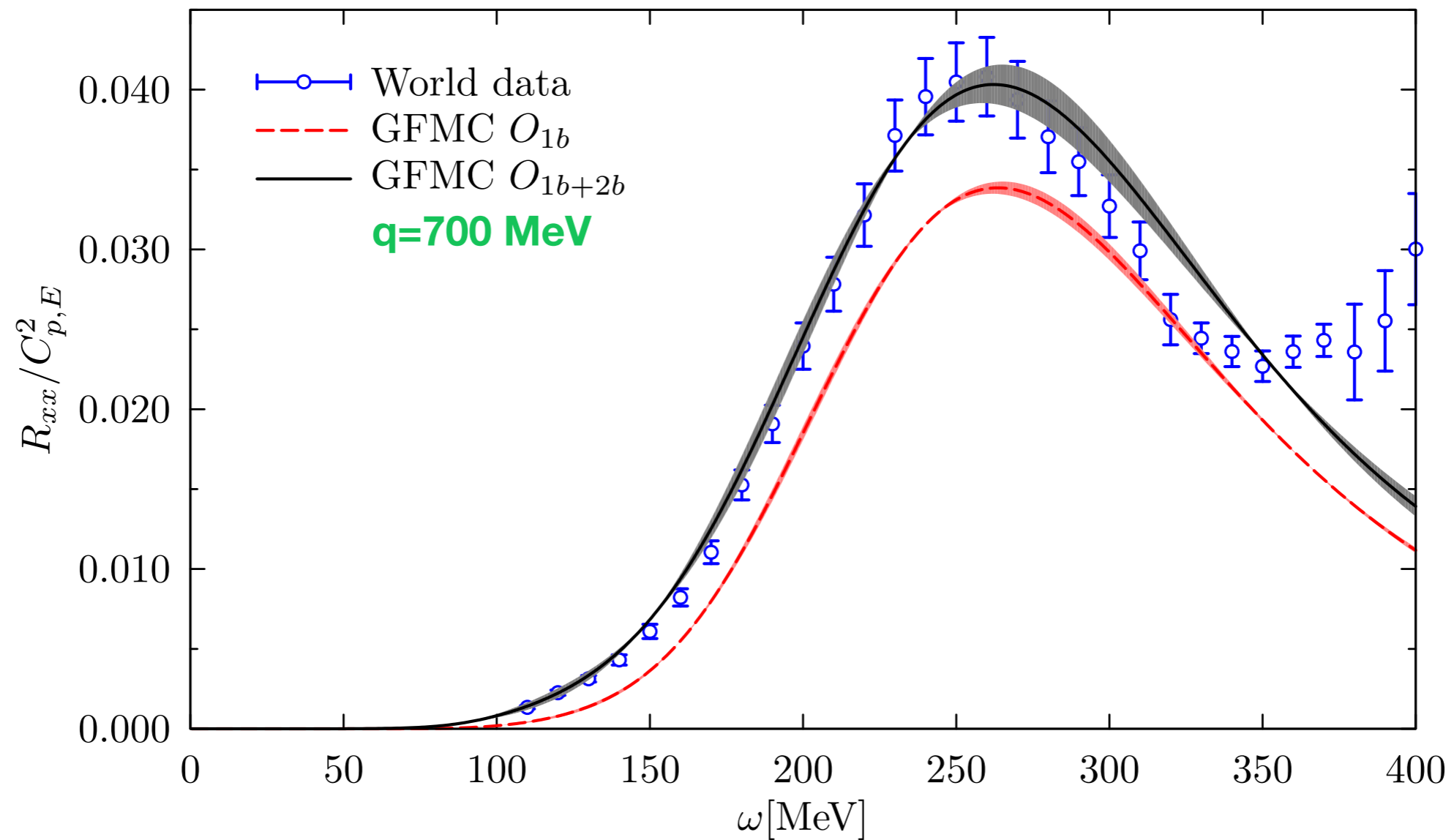
^4He electromagnetic response

Two-body currents significantly enhance the transverse response function, not only in the dip region, but also in the quasielastic peak and threshold regions.



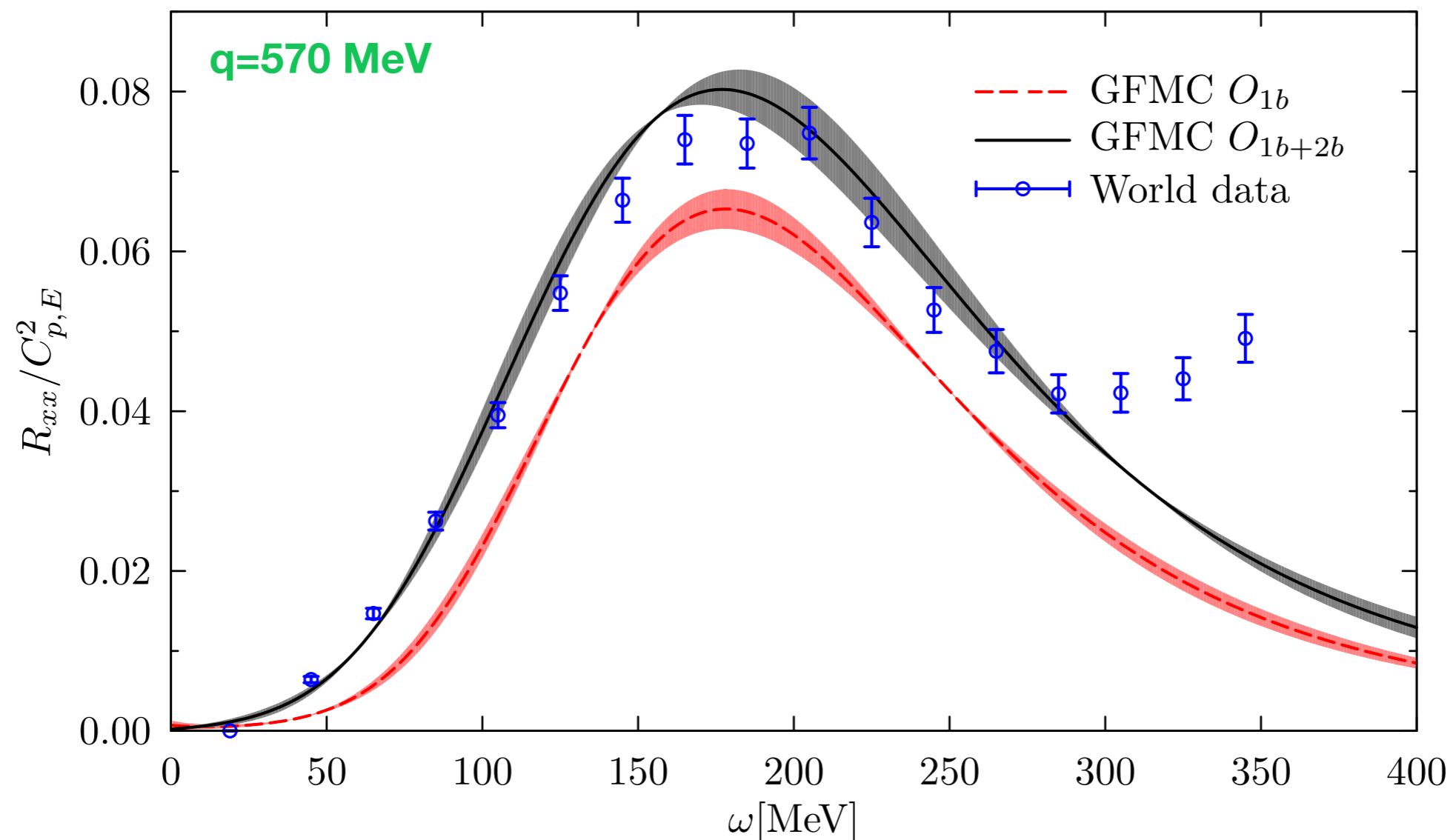
^4He electromagnetic response

Two-body currents significantly enhance the transverse response function, not only in the dip region, but also in the quasielastic peak and threshold regions.



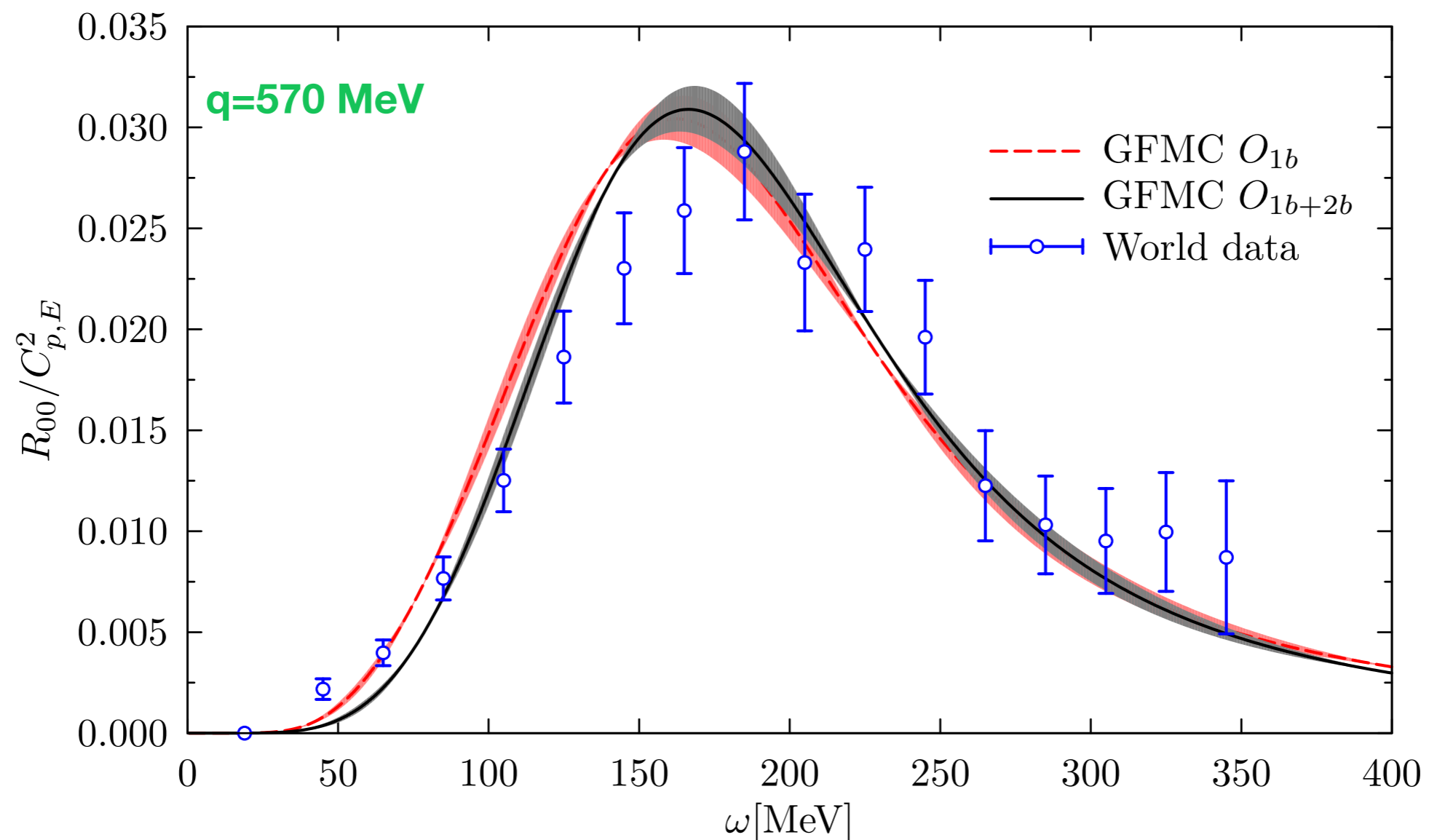
^{12}C electromagnetic response

- We were recently able to invert the electromagnetic Euclidean response of ^{12}C . This is the first ab-initio calculation of the electromagnetic response of ^{12}C !
- Very good agreement with experimental data once two-body currents are accounted for!



^{12}C electromagnetic response

- We were recently able to invert the electromagnetic Euclidean response of ^{12}C . This is the first ab-initio calculation of the electromagnetic response of ^{12}C !
- Very good agreement with experimental data. Small contribution from two-body currents



Large momentum-transfer regime

Quantum Monte Carlo & the spectral function

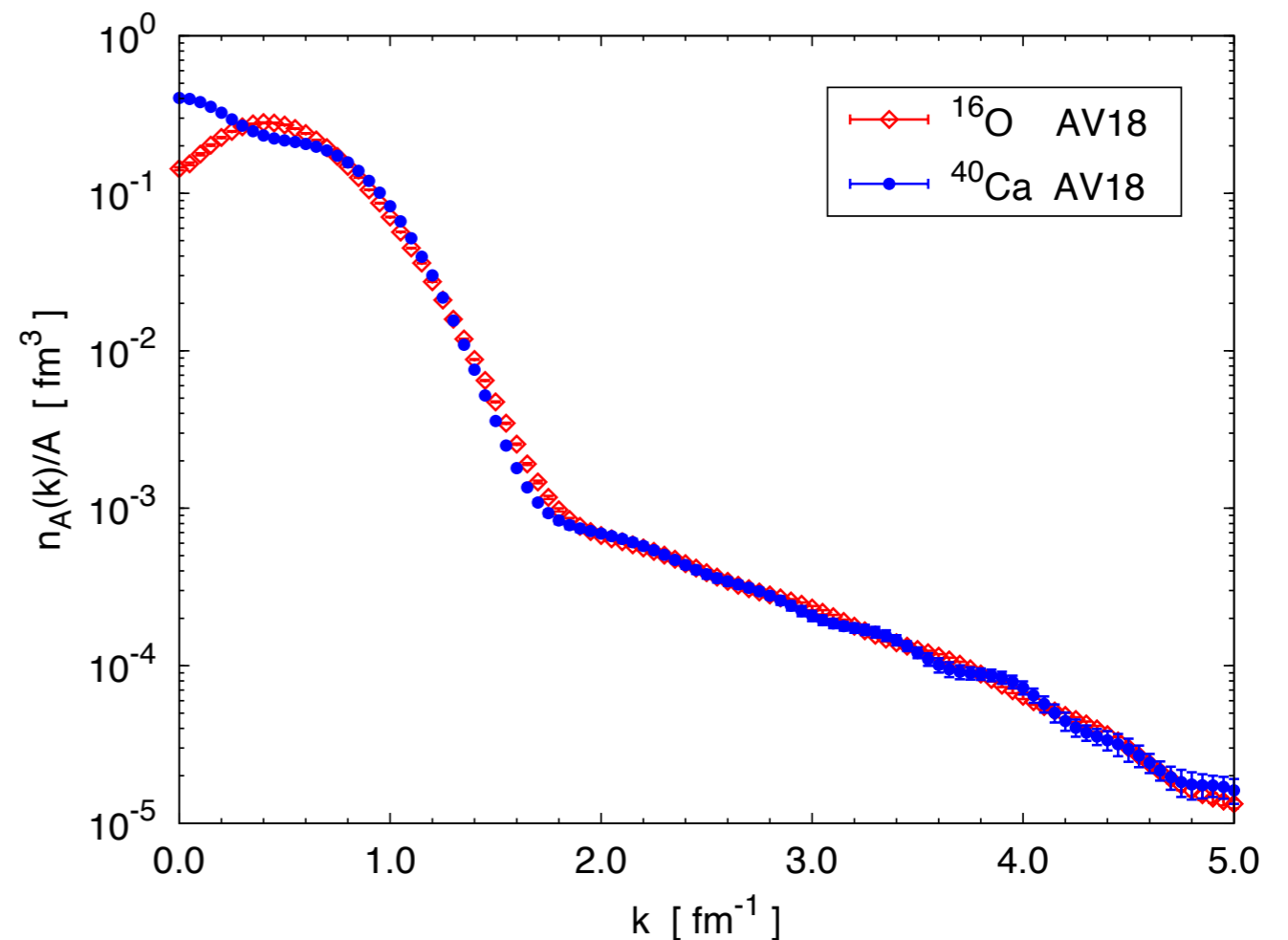
In the relativistic regime, the final state includes at least one particle carrying large momentum, whereas the initial nuclear state is still an eigenstate of the nuclear Hamiltonian.

The spectral function formalism allow one to circumvent the difficulties associated with the relativistic treatment of the nuclear final state and current operator, while at the same time preserving essential features (such as correlations) inherent to the realistic description of nuclear dynamics

The sum rule of the spectral function corresponds to the momentum distribution

$$\int dE P(\mathbf{k}, E) = n(\mathbf{k})$$

The momentum distribution of nuclei as large as ^{16}O and ^{40}Ca has been computed using QMC fully accounting for the correlations of the nuclear ground state



Conclusions

- For relatively large momentum transfer, the two-body currents enhancement is effective in the entire energy transfer domain.
- We have computed the electromagnetic and neutral-current Euclidean response of ^{12}C . The agreement of the former with experimental data is remarkably good.
- ^4He and ^{12}C results for the electromagnetic response obtained using Maximum Entropy technique are in very good agreement with experimental data.
- Fruitful interplay between Green's function Monte Carlo and the spectral function approach. Both are based on the same model of nuclear dynamics.

Current developments

- We are implementing charged-current transition operator in GFMC and the corresponding Euclidean responses will soon be computed.
- Cluster variational Monte Carlo calculations of the energy weighted sum rules of the spectral function for nuclei as large as ^{40}Ca will be carried out. Crucial interplay with (e,e') experiment on Argon at JLab.
- We plan to compute the Laplace transform of the spectral function using GFMC. Maximum-entropy technique may well be used to obtain the real spectral function.

$$P^{(E)}(\mathbf{k}, \tau) = \langle 0 | a^\dagger(\mathbf{k}) e^{-(H-E_0)\tau} a(\mathbf{k}) | 0 \rangle$$

Thank you

Maximum entropy algorithm

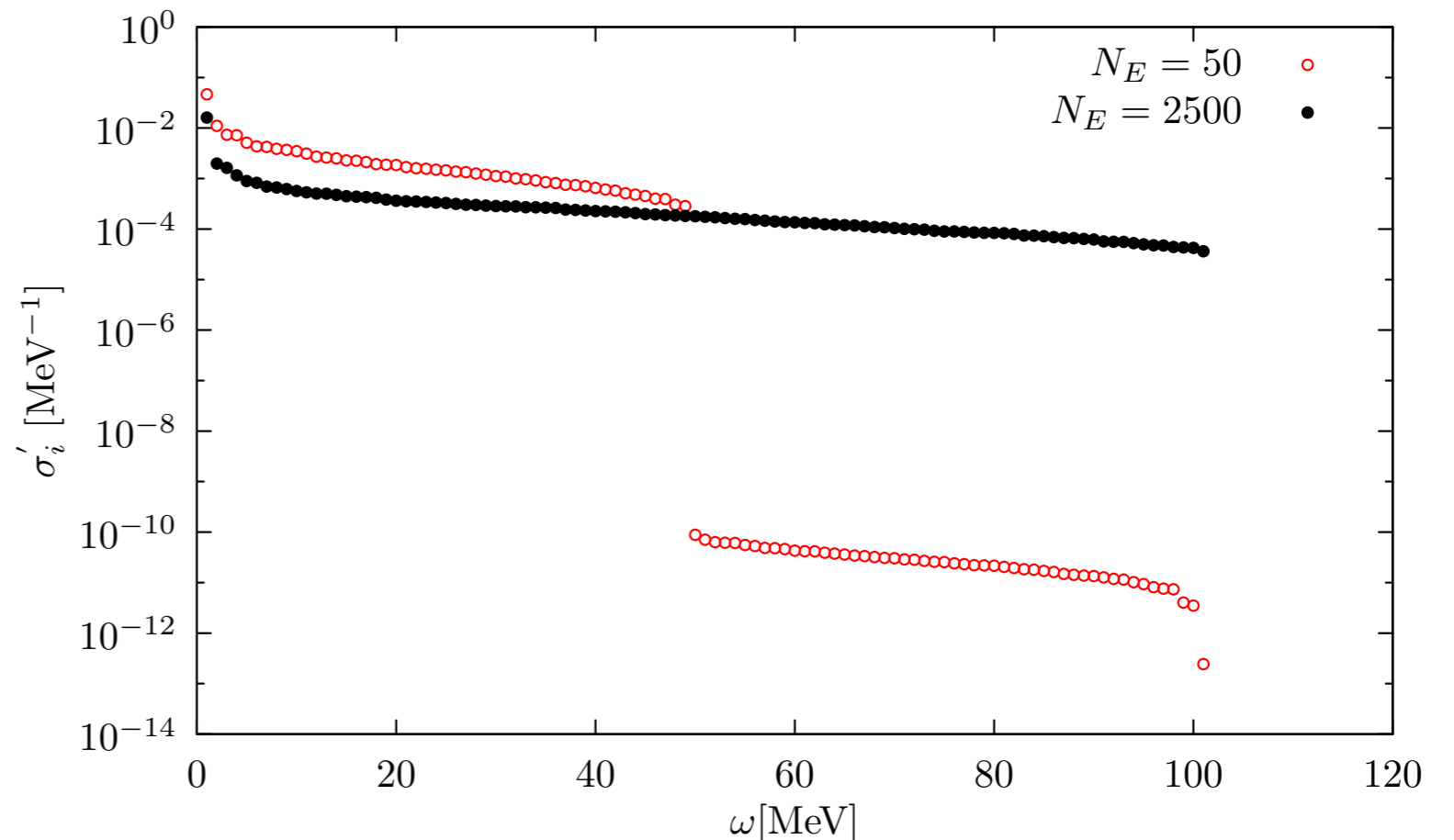
We estimate the mean and the covariance matrix from N_E Euclidean responses

$$\bar{E}(\tau_i) = \frac{1}{N} \sum_n E^n(\tau_i) \quad C(\tau_i, \tau_j) = \frac{1}{N(N-1)} \sum_n (\bar{E}^n(\tau_i) - E^n(\tau_i))(\bar{E}^n(\tau_j) - E^n(\tau_j))$$

- The covariance matrix in general is NOT diagonal, and it is convenient to diagonalize it

$$(\mathbf{U}^{-1} \mathbf{C} \mathbf{U})_{ij} = \sigma_i'^2 \delta_{ij}$$

- If N is not sufficiently large, the spectrum of the covariance eigenvalues becomes pathological.



Maximum entropy algorithm

- The likelihood is defined in terms of the covariance matrix

$$\chi^2 = \sum_{i,j=1}^{N_\tau} (\bar{E}_i - E_i) (C^{-1})_{ij} (\bar{E}_j - E_j) \quad E_i = \sum_{j=1}^{N_\omega} K_{ij} R_j$$

- We rotate both the data and the kernel in the diagonal representation of the covariance matrix

$$\mathbf{K}' = \mathbf{U}^{-1} \mathbf{K} \quad \bar{\mathbf{E}}' = \mathbf{U}^{-1} \bar{\mathbf{E}} \quad \longleftrightarrow \quad (\mathbf{U}^{-1} \mathbf{C} \mathbf{U})_{ij} = \sigma_i'^2 \delta_{ij}$$

- The likelihood can be written in terms of the statistically independent measurements and the rotated kernel

$$\chi^2 = \frac{1}{N_\tau} \sum_i \frac{(\sum_j K'_{ij} R_j - \bar{E}'_i)^2}{\sigma_i'^2}$$

Maximum entropy algorithm

Maximum entropy approach can be justified on the basis of Bayesian inference. The best solution will be the one that maximizes the conditional probability

$$Pr[R|\bar{E}] = \frac{Pr[\bar{E}|R] Pr[R]}{Pr[\bar{E}]}$$

- The evidence is merely a normalization constant

$$Pr[\bar{E}] = \int \mathcal{D}R Pr[\bar{E}|R] Pr[R]$$

- When the number of measurements becomes large, the asymptotic limit of the likelihood function is

$$Pr[\bar{E}|R] = \frac{1}{Z_1} e^{-L[R]} = \frac{1}{Z_1} e^{-\frac{1}{2}\chi^2[R]} \quad \chi^2 = \frac{1}{N_\tau} \sum_i \frac{(\sum_j K'_{ij} R_j - \bar{E}'_i)^2}{\sigma_i'^2}$$

Limiting ourselves to the minimization of the χ^2 , we implicitly make the assumption that the prior probability is important or unknown.

Maximum entropy algorithm

Since the response function is nonnegative and normalizable, it can be interpreted as a probability distribution function.

The principle of maximum entropy states that the values of a probability function are to be assigned by maximizing the entropy expression


$$S[R] \equiv - \int d\omega (R(\omega) - D(\omega) - R(\omega) \ln[R(\omega)/D(\omega)]) \quad \longleftrightarrow \quad D(\omega): \text{Default model}$$

The prior probability then reads

$$Pr[R] = \frac{1}{Z_2} e^{\alpha S[R]}$$

and the posterior probability can be rewritten as

$$Pr[R|\bar{E}] = \frac{e^{-Q[R]}}{Z_1 Z_2 Pr[\bar{E}]} \quad \longleftrightarrow \quad Q[R] \equiv \frac{1}{2} \chi^2[R] - \alpha S[R]$$



Regularization parameter

^4He electromagnetic response

The enhancement is driven by process involving one-pion exchange and the excitation of the Delta degrees of freedom

